Pergamon

*Calphad*, Vol. 24, No. 1, pp. 55–94, 2000

0364-5916/00/$ - see front matter

PII: S0364-5916(00)00015-8

**Workshop on**

APPLICATIONS OF COMPUTATIONAL THERMODYNAMICS

Schloß Ringberg, November 30 - December 5, 1997

---

**Joint Report from**

# Groups 4: USE OF THERMODYNAMIC SOFTWARE IN PROCESS MODELLING

**and**

# Group 5: NEW APPLICATIONS OF THERMODYNAMIC CALCULATIONS

**Group Members**

**Group 4**

**Ursula R. Kattner** (Group Leader)
NIST, Gaithersburg, MD, USA

**Gunnar Eriksson**
Aachen, Germany

**Iris Hahn**
Siemens AG, München, Germany

**Rainer Schmid-Fetzer**
TU Clausthal-Zellerfeld, Germany

**Bosse Sundman**
KTH, Stockholm, Sweden

**Varghese Swamy**
CSIRO, Clayton, Australia

**Armin Kussmaul** (Assistant)
MPI Stuttgart, Germany

**Group 5**

**Philip J. Spencer** (Group Leader)
RWTH Aachen, Germany

**Tim J. Anderson**
UF, Gainesville, FL, USA

**Tim G. Chart**
Chart Associates, Ashford, UK

**André Costa e Silva**
UFF, Volta Redonda, Brasil

**Bo Jansson**
SECO Tools AB, Fagersta, Sweden

**Byeong-Joo Lee**
KRISS, Taejon, South Korea

**Mikael Schalin** (Assistant)
KTH, Stockholm, Sweden

Received on 30 November 1999

## 1. Introduction

The strongly related nature of the topics allocated to Groups 4 and 5 was such that a close interaction between the two groups appeared essential at all stages of the discussions and for this reason the groups amalgamated. A joint decision was made as to which emerging or potential new applications should be selected for deeper analysis. This would include definition of requirements with respect to measurement/estimation/calculation of missing data and on this basis, the necessary software to treat the application would be envisaged.

Thermodynamic calculations and simulations based on critically evaluated data are widely used as a basic tool in the development and optimization of materials and processes of many different types. The practical reasons for carrying out such computational studies are self-evident. If the calculations involved can be made sufficiently reliable, considerable time and costs can be saved in experimental development work.

To assist these calculations, a number of thermodynamic databases as well as different computational software have found wide application. Their use enables information to be obtained very rapidly and inexpensively on process conditions necessary to achieve a product of the required property with minimum wastage of energy and materials.

Many materials in use today are composed of several deliberately alloyed constituents to achieve desired mechanical and/or physical properties. A full thermodynamic description of the phases constituting these materials must form part of the calculation procedure to enable full account to be taken of reactions such as those between an alloy melt and a slag phase, or those involved in forming precipitated phases in a multicomponent alloy, or in vapour deposition of complex coatings on an alloy substrate.

Apart from the capability of simulating processes of interest, whereby a process can be improved by determination and optimization of the critical parameters, the speed of calculation now available offers a real possibility to use the calculations for process control in certain cases - for example, to control the composition of the gas atmosphere in carburizing or nitriding processes.

Thermodynamic calculations are finding particularly important use as the basis for a directed measurement programme. By proceeding hand-in-hand, calculation and experiment result in much more rapid and reliable progress than that associated with widely applied trial-and-error development methods.

In more recent thermodynamic software developments, the influence of kinetic effects on calculated thermodynamic equilibria is being taken into account, *e.g.* by introducing descriptions of diffusion phenomena into the calculations [90And, 92And], or by incorporating rates of reaction [95Kou].

Typical examples of processes and materials which have been and are being improved and developed with the help of thermodynamic calculations are presented below.

## 2. State of the art

The state of the art in the field of applying thermodynamics to materials design and processing as well as to other industrial, environmental and geological processes is summarized below. This is intended to give an idea of the broad scope of this growing field and not meant to be an exhaustive literature survey. It is useful to classify the applications of materials thermochemistry in four categories. These depend on how much quantitative kinetic data are involved or coupled to the thermodynamic software and data.

### 2.1 Direct applications

The direct applications of phase diagrams or thermodynamic equilibrium calculations started about a century ago with the first understanding of alloying behaviour, microstructure development and metallurgical reactions. These applications are far from being "old-fashioned", though. Today we are able to apply quantitative phase equilibrium calculations in multicomponent multiphase materials to the development of technical alloys [96Gus], and also to the optimization of near-equilibrium processing conditions [93Kub]. This goes as far as setting he

electronic carrier concentration in CdTe semiconductors by annealing at appropriate partial pressures of Cd [98Che].

The vast majority of examples given in **Table 1** belong to this category. Many successful applications rely on the fact that the actual process conditions are close to equilibrium, as in the case of the highly disperse and high temperature steel converter process or other activated processes. The calculations of solidification paths under equilibrium conditions or even with the popular Scheil model are also considered as very useful direct applications, since no kinetic data are needed when completely blocking the solid state diffusion in the Scheil model.

However, even materials processing far from equilibrium (such as splat cooling, mechanical alloying, annealing of reactive thin film multilayers) requires a sound knowledge of thermodynamic data of equilibrium and metastable phases [93Gen, 94Bor, 95Bus]. Once these data are available, modern software can calculate the driving forces for metastable phase formation or even complete metastable phase diagrams to provide "road maps" for the engineering of these advanced materials.

### 2.2 Coupling with steady state reactor modelling

A reactor like an electric arc furnace can be modeled by splitting it up to a certain number of reactor stages. Within each stage a (local) equilibrium calculation can be performed using the thermodynamic data set of the materials system. In addition to the number of stages one has to specify the feed phases (amounts, compositions, temperatures, input stages), the enthalpy supplied/evolved or the temperature imposed on each stage, pressure of each stage and optionally distribution coefficients of phases which may simulate kinetic inhibitions. Steady-state equilibrium is attained by equilibrium calculations where the output of one stage is used as input of the next stage in co- and counter-current flow reactors. Convergence is usually achieved with reasonably estimated initial values for each stage obtained by separate equilibrium calculations.

A nice example is the production of metallurgical grade silicon in an electric arc furnace, where the ChemSage software was used [96Eri]. It should be noted that actual kinetic data (diffusion, fluid flow, ...) of the materials' system are not necessary in this approach. The optionally imposed phase distribution coefficients are not considered as detailed kinetic data. As an example the imposed fraction of $NH_3$ in MOCVD growth of nitride semiconductors in a simple one-stage reactor is given [96Kou].

### 2.3 Coupling with micro-kinetics

Applications governed by micro-kinetics are mostly solid state transformations, growth or dissolution of precipitates, reactions at solid/solid interfaces and so on. Fluid flow and heat transfer problems do not occur or are irrelevant. Thermal equilibrium is often assumed since thermal diffusion is much faster compared to species diffusion in solids.

The framework of multicomponent (multiphase) diffusion is used, which requires the full data set of diffusion coefficients of all species in all phases. Possibly even the nucleation may be included with an appropriate model. The phase growth is usually assumed to be diffusion controlled. Appropriate software is designed with analytical and/or numerical methods.

Thermodynamic software and data sets are called as a "subroutine" to provide local equilibrium calculations and the driving forces for diffusion. These calculations yield quantitative data at locally prevailing temperature, pressure, composition or chemical potentials. It is advisable to use the "subroutine" approach and not to fully integrate the thermodynamic and diffusion software. The thermochemical and phase equilibrium calculations in real systems may become rather complex and should be thoroughly tested separately for internal consistency and accuracy.

A prominent example of this approach is the DICTRA software [92Agr], just a few applications are mentioned here for the multicomponent diffusion in steel [92Agr, 96Agr].

### 2.4 Coupling with macro-kinetics

Comprehensive simulation of dynamic, macro-scale processes involving fluid flow constitute the highest level of complexity and requirement of additional system data. An example is the simulation of technical alloy casting, where in up to three-dimensional simulation of the moving mushy solidification front, void formation at hot spots and macro-segregation may be covered. The other aspect of microsegregation, dendrite shape formation and ultimately the development of microstructure is still mostly treated separately. Both aspects require thermodynamic equilibrium calculations at the core of appropriate process simulation software that tries to solve the simultaneous mass- heat- and momentum-transfer with moving phase boundaries.

Such process simulation software is working in the framework of computational fluid dynamics (CFD) or flow-sheeting. Depending on the complexity, the full set of data for the macro-kinetic description of the system may be needed, possibly including the micro-kinetic data. The current challenge is to incorporate exact thermodynamic phase equilibrium calculation into commercial software packages like Phoenics, Fluent, Aspen, Process and so on. To this aim a general software interface TQ (ChemApp) has been developed that allows to call the most widely used Gibbs energy minimizers as a subroutine [94Eri]. This is detailed in section 4.

An example for the casting process, where the link to thermodynamic software was programmed with another sofware interface, is given by [97Ban], see also the section on solidification. If also the simulation of mushy zone is included in an attempt to couple macro- and micro-kinetics, the computation time becomes a major issue [97Sch].

Another problem is that the thermodynamic software subroutine has to be 100% reliable and convergent for each individual complex equilibrium calculation even if starting from unrealistic initial values set by the process software. Envisaging about $10^5$ calls of the thermodynamic subroutine, a single failure return would obstruct the process simulation.

**Table 1: Some examples for applications of thermodynamics to processes**

| Processes | Materials | References |
|---|---|---|
| bulk metal production, recycling:<br>pyrometallurgical and<br>hydrometallurgical processes | <br>iron and steel, slags,<br>refractories,<br>non-ferrous metals | 93Kub, 96Tur<br>74Sig, 87Deo, 96Sui<br><br>96Bar2, 96Eri, 96Kor |
| ceramics & powder metallurgy:<br>sintering, infiltration, reaction<br>sintering | metals, intermetallics,<br>ceramics,<br><br><br>cermets | <br>91Pet, 95Tie, 96Hil2, 96Sei1,<br>96Sei2, 98Sei,<br>98Sch<br>98Zen |
| materials design, alloy<br>development | high speed steel,<br>cemented carbide,<br>Mg-alloy | 96Gus<br>96Fer<br>98Buc |
| casting, solidification:<br><br>- continuous casting<br>- die and mold casting | metals, alloys | 89Rap, 95Boe, 96Kat, 97Kra,<br>97Sch<br>92Bat, 95Ste<br>97Ban |
| heat treatment:<br>homogenization,<br>quenching, age hardening,<br>thermomechanical processing | mostly alloys | <br>92Agr<br>96Agr<br>95Tho |

| Processes | Materials | References |
|---|---|---|
| surface coating: | hard materials, corrosion resistant materials | 86Sau, 90Spe, 93Sto, 98Spe, 96Vah |
| - chemical vapour deposition | (Ti,Al)(C,N), $Al_2O_3$, $WSi_2$ | 96Ric |
| - physical vapour deposition | (Ti,Al)(C,N) | |
| - dip coating | Zn | |
| surface modification: | metals, alloys | |
| - nitridation | + $NH_3$, N | |
| - carburization | + $CH_4$, .. | 96Hol |
| - cementation | + Al-carrier,... | 98Sch |
| single crystal growth | mostly semiconductors | |
| - bulk from liquid | | |
| Czochralski, floating zone, | Si | |
| liquid encapsulated Chochralsi, | GaAs | 93Wen |
| Bridgman | CdTe, SiC | |
| - bulk from gas (vapour transport) | | |
| - epitaxy from liquid | compound semiconductors | 72Pan |
| liquid phase epitaxy, recrystallization | | |
| - epitaxy from gas | Si, compound semiconductors | 96Kou |
| vapour phase epitaxy, metal-organic chemical vapour depositon | | |
| - activation annealing, carrier concentration engineering | semiconductors | 89Sha, 95Ito, 98Che |
| joining: | metal/metal | 93Hum, 97Lee1, |
| soldering, welding, brazing, | metal/ceramic | 96Bha, 96Pau |
| isothermal solidification, | intermetallic/intermetallic | 96Ann |
| transient liquid phase bonding | semiconductor die bonding | 96Sch |
| interface engineering: | | 90Loo |
| - contact formation to semiconductors | metal/semiconductor | 92Cor, 94Han, 95Goe, 95Lin, 95Moh |
| - composites, fibre/matrix or particle/matrix interactions | metal/ceramic | 92Li, 97Lee2 |
| | ceramic/ceramic | 96Kao |
| materials processing far from equilibrium: rapid solidification, mechanical alloying, multilayer thin films | metastable and amorphous alloys | 90Gio, 93Gen, 94Bor, 95Bus |
| corrosion: | | |
| - high temperature corrosion (bulk and coatings) | superalloys, steel | 96Bar1, 96Hil1 |
| - corrosion in aqueous media | ceramics | 96Nic |
| environmental applications: emission control of toxic effluents in | | |
| -- waste incineration | waste | |
| -- ore sintering | iron ore | 97Eri |
| nuclear reactor safety | nuclear core materials | 96Bal |

| Processes | Materials | References |
|---|---|---|
| geological processes: | natural geologic materials | |
| natural waters, brines, soil solutions | | 87Wea, 93Fle |
| aqueous alteration of asteroids | | 89Zol |
| hydrothermal alteration | | 97Tut, 98McC |
| ore-forming processes | | 87Bri |
| metamorphic reactions | | 93Spe, 91Ker |
| magmatic processes | | 97Ghi, 90Nie |
| mineral physics | | 92Ita, 96Sax |

## 3. Current and emerging applications

### 3.1 Electronic materials

The processing of electronic materials is an area where thermodynamics has made important contributions. This has come about in part because many of the processes used to grow semiconductors involve near equilibrium fluid-solid interfaces. As a result the design and analysis of these processes often specify equilibrium boundary conditions. This is possible because processes are typically operated in the mass transfer limited regime to improve reproducibility (*i.e.*, avoids strong temperature sensitivities usually associated with kinetically limited processes). Examples include the solid-liquid interfaces found in bulk crystal growth processes and in liquid phase epitaxy of compound semiconductors, the vapour-solid interface present in chemical vapour deposition, and the solid-solid interface encountered in metal contact formation schemes. In addition to coupling equilibrium boundary conditions with detailed process models, qualitative trends can also be ascertained by the application of more straightforward equilibrium models. This approach is much simpler compared to detailed models that require solution of the 3-dimensional, time-dependent equations of change with chemical reaction.

A simple example involves the deposition of Al onto Si to serve as an electrical contact [88And]. The limited solubility of Si in Al can lead to "spiking" of Al through a p-n junction to short circuit a device under certain processing conditions. This spiking occurs by the preferential dissolution of Si into the Al metallization layer along an extended defect. Upon cooling the solubility of Al in Si decreases to produce a spike of conductor through the semiconductor. This phenomenon is easily suppressed by simply co-depositing Al with a small amount of Si. The amount of Si to add and the permitted processing temperature range can be reasonably estimated by examining the Al-rich segment of the Al-Si phase diagram.

Another example is the segregation of dopants during bulk crystal growth of semiconductors. Reasonable predictions of the axial variation of dopants in Bridgman grown GaAs for example are given by assuming an equilibrium distribution of the dopant across the growth interface and a description of the dynamic state of the melt to provide mass transfer rates. For some growth chamber designs and imposed temperature gradients, the melt is stagnant and a simple diffusion limited transport model works well. The other extreme of a well-mixed liquid can be approximated when intense buoyancy driven convection is present. Again an equilibrium boundary condition at the melt-crystal interface gives a reasonable description of the dopant axial variation.

A similar process that motivated much of the early phase equilibrium work in compound semiconductors is the thin film deposition process liquid phase epitaxy [89And]. In this process a solution rich in the lowest vapour pressure element is brought into contact with a substrate. The temperature is then decreased below the saturation temperature to drive slow solidification. A diffusion-limited transport model with equilibrium established at the growth interface accurately describes the film composition and growth rate.

Equilibrium models of chemical vapour deposition have proved useful for rapidly exploring the influence of deposition parameters on the growth characteristics [83And, 85Hes]. As an example, Figure 3.1.1 shows the effect of varying the inlet Ge/Ge+Si molar ratio on the film composition at a constant Cl/H ratio and various growth temperatures [87Cha]. It is clear that there is a region in which the film composition is extremely

sensitive to the inlet ratio and growth temperature, and should be avoided if films of uniform composition are to be grown. Equilibrium calculations also predict the composition of compound semiconductor films deposited by metal-organic chemical vapour deposition (MOCVD) when operated in the mass transfer limited regime.

Figure 3.1.2 compares predicted and actual film compositions of $ZnS_xSe_{1-x}$ films as a function of the inlet Se/Se+S molar ratio. The critical information that is required for this calculation is the solid solution phase thermodynamics. Unfortunately no thermodynamic property data exist for the solid solution. An estimate of the enthalpy of mixing, however, was obtained from the measured bandgap energy. As shown in Figure 3.1.2 this estimate predicts the film composition reasonably well.

As a final example, Figure 3.1.3 shows some measured hole concentrations in Zn-doped InP grown by MOCVD as a function of the inlet diethyl-Zn partial pressure. Carrier concentrations were measured by Hall measurements and the total Zn content determined by SIMS analysis. As can be seen the Zn concentration exceeds the hole concentration at high inlet Zn partial pressure. To model this process the energy, momentum, and species balance equations were solved for the specific reactor design used in the experiment assuming equilibrium at the growth interface. The calculation gave the partial pressure of Zn, In and P species in the vapour at the growth interface from which the growth rate could be computed. To give

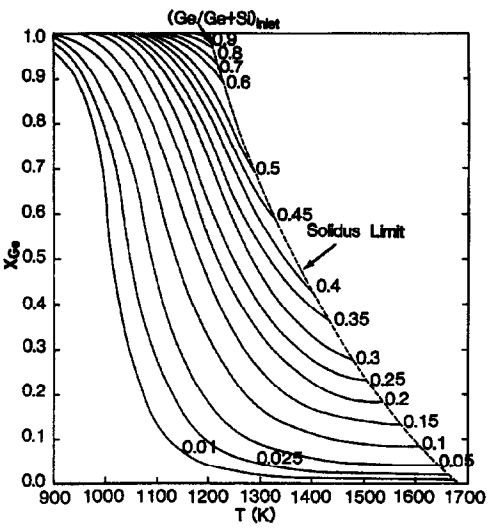


FIG. 3.1.1
Equilibrium Ge mole fraction in solid Si-Ge solid solutions deposited by chloride CVD as a function of deposition temperature for values of the Ge/Ge+Si inlet molar ratio at a fixed Cl/H ratio of 0.01.

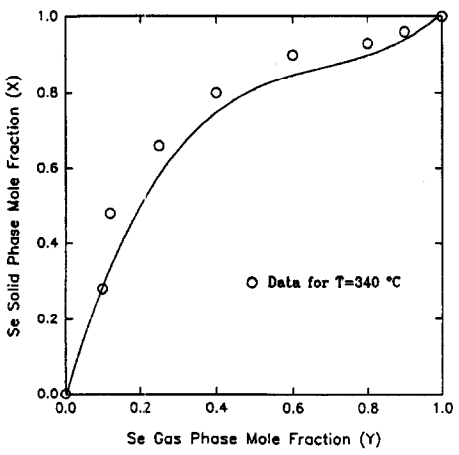


FIG. 3.1.2
Equilibrium fraction of ZnSe in the solid solution ZnS-ZnSe deposited by MOCVD at 340 °C as a function of the Se/Se+S inlet gas phase molar ratio.

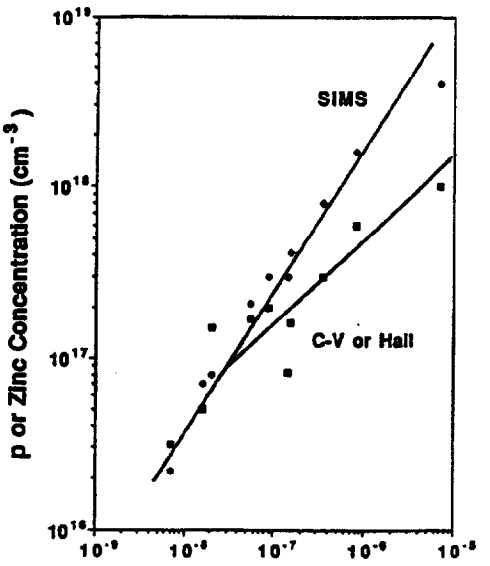


FIG. 3.1.3
Measured hole concentration and total Zn incorporation as a function of the inlet DEZn partial pressure. Solid line is predicted by model.

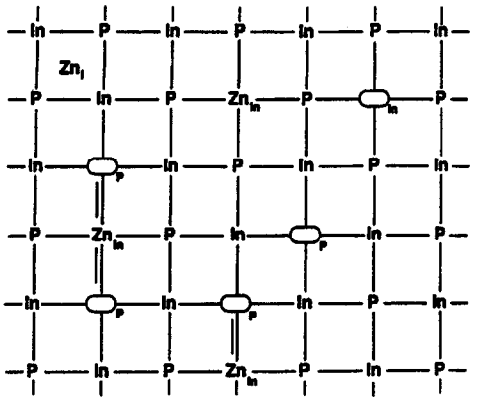


FIG. 3.1.4
Schematic of point defects assumed in model.

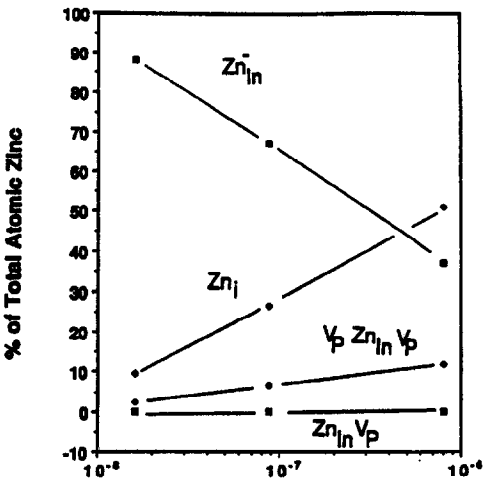


FIG. 3.1.5
Equilibrium distribution of incorporated Zn during MOCVD of InP at conditions identical to data shown in Figure 3.1.3

insight into the incorporation of Zn into InP, a point defect model shown schematically in Figure 3.1.4 was developed that included Zn substitution on both In vacancy and interstitial sites, as well as forming two complexes. The vapour phase composition produced by the detailed reactor model was then assumed to be in equilibrium with the defective InP. The solid lines shown in Figure 3.1.3 are the predicted Zn incorporation extent and hole concentrations. At high Zn partial pressure the hole concentration increases which decreases the In vacancy concentration. Thus relatively more electrically inactive interstitial Zn is incorporated, explaining the SIMS Zn concentration exceeding the measured hole concentration or equivalently the electrically active Zn. Figure 3.1.5 shows the quantitative distribution of Zn between the interstitial and substitutional sites and their variation with the Zn partial pressure at the growth interface. The complexes are not dominant species but are required to explain the higher solubility limit.

The identification of emerging and potential applications can be difficult since the field is rapidly changing. Areas that are currently emerging with a major economic potential include visible and UV light emitting devices, flat panel displays, high power and temperature electronics, thin film photovoltaics (PV) [96Cha], and, of course, higher speed Si-based integrated circuits. Other areas under intense research but with less clear potential for significant commercialisation include high $T_c$ superconductor applications, integrated photonic devices, and organic optoelectronic devices.

It is also evident that the collection of process technologies used to fabricate these emerging devices will largely remain the same. The growth of substrates will likely be performed by melt growth (Czochralski and Bridgman configurations) or vapour phase transport processes. The deposition of epitaxial films will likely be dominated by chemical vapour deposition (CVD) and, for research demonstration, by molecular beam epitaxy (MBE). Dielectric materials will be deposited by CVD, plasma assisted processes, and sputtering, while metal deposition will be by CVD and physical processes such as evaporation and sputtering. Dopant incorporation will probably take place *in situ* during deposition or *ex situ* by ion implantation. A significant change in the lithographic process is expected as the minimum feature size decreases below 0.2 microns. It is thus expected that the conceptual processes will remain in place with only changes in process chemistry and scale/throughput required to meet future challenges.

The opportunities that exist for applying computational thermodynamics to these emerging areas are best summarised by the future materials needs for device applications. The semiconductor materials can be classified according to their position in the periodic table. For the column IV materials some needs that are emerging include thinner and/or higher dielectric constant gate dielectric materials and higher conductivity interconnects

(*e.g.*, Cu conductors with suitable contact schemes). The alloy $Si_xGe_{1-x}$ is also a promising semiconductor that allows variation of the physical properties of Si. There is interest in adding carbon to form the ternary alloy $Si_xGe_yC_{1-x-y}$ to compensate for the increased atomic radius of Ge. The solubility of C in $Si_xGe_{1-x}$ is not known but expected to be small. Also the spinodal line accounting for the strain energy or the phase diagram constrained to the amorphous state would be of interest since metastable films will likely be grown on Si substrates. Considerable research has already been devoted to the development of thin film diamond deposition and the extent of commercialisation is yet to be determined. The recent interest of SiC substrates grown by vapour phase transport has motivated intense research in this material for high power and temperature devices. The growth process needs further improvement, as well as doping and metallization schemes. Each of these problem areas could benefit from equilibrium analyses.

The column III-V semiconductors have been the objects of sustained research for three decades [90Hol1]. This effort has resulted in the commercialisation of specialised discrete devices (*e.g.*, lasers, LEDs, microwave devices, IR detectors) and, more recently, high speed integrated circuits. Most of the commercial applications have been based on the AlGaAs pseudobinary solid solution (*e.g.*, red lasers for CD players and bar scanners) and the InGaAsP quaternary (*e.g.*, 1.3 micron optical fibre transmission sources). More recently Sb containing materials have been proposed for IR detector structures and AlGaInP for visible emitters. The group III nitrides are under intense investigation at this time for both visible emitter and high power and temperature device applications, and are just beginning to be commercialised.

The group II-VI materials are also of interest, although far from the extent of commercialisation found with Si and the III-V materials. HgCdTe is of interest for IR detectors, ZnS for electroluminescent displays, CdTe for PV applications, and ZnSe-based materials for visible emitters. Many of the II-VI semiconductors, however, are competing with other materials for the same application. The phase equilibrium and thermochemistry of most of the III-V and to a lesser degree the II-VI materials are relatively well defined. Ansara *et al.* [94Ans] recently assessed the III-V systems in a consistent manner. The experimental database for the solid solutions, however, is extremely limited. The solid solution behaviour is usually ascertained from an optimisation of the high temperature pseudobinary phase diagram or the low vapour pressure and temperature corner of ternary diagrams. As a result the solution model parameters are correlated with each other as well as those for the liquid phase.

These selected examples show how knowledge of phase equilibrium can contribute to our understanding of a variety of processes. One can use phase diagrams to predict the formation of possible phases, establish a boundary condition in a detailed process model, or calculate chemical equilibrium to understand reacting systems. Equilibrium calculations are relatively easy to perform with the software packages now available using the property databases or estimations procedures developed over the last decade [85Ase].

### 3.2 Charged defects

The complexity of materials chemistry is less essential for elemental semiconductors, and this is the reason why the applications in this field focus on compound semiconductors. The technologically most important thermodynamic parameter of a compound semiconductor is the electronic carrier concentration. This property can vary by orders of magnitude over small changes in stoichiometry of the compound and determines the intrinsic conductivity. In the processing of these materials, these small stoichiometric changes can be controlled via the chemical potentials of the components in a contacting gaseous or liquid phase. Therefore, it is crucial to develop a consistent thermodynamic description of the material system, that covers the chemical potentials of all species, including electrons and holes, and all the phase equilibria.

A supreme way to achieve this consistency is to construct models for the integral Gibbs energy of all phases using the CALPHAD approach. An example is given for the Cd-Te system [98Che]. The most complex phase is the semiconducting solid solution CdTe. In this case the various point defects in CdTe are described by an extension of the compound energy formalism (CEF), where electrons and holes occupy dummy sublattices for the conduction and valence bands. They interact with the charged defects like vacancies, substitutional or interstitial atoms that are introduced in the perfect CdTe crystal. As a result, the concentration of all defects ($e^-$, $h^+$, $Va_{Cd}$, $Va_{Cd}^{-2}$, $Te_{Cd}$, $Va_{Te}$, $Va_{Te}^{+2}$, $Cd_{Te}$, $Cd_I$, $Cd_I^{+2}$) can be consistently calculated at any temperature and cadmium (tellurium) pressure or composition. The very same model provides a quantitative description of the entire phase diagram, including the minute deviation from stoichiometry (± 0.01 at.%) in the CdTe solid solution [98Che]. A

drawback of the actual model used in this case (CEF) is that it formally introduces up to 192 parameters which have first to be condensed by empirical considerations to a reasonable number of 4 (max 10) coefficients. These are then optimized using the CALPHAD approach considering all experimental data (phase equilibria, thermodynamic data and physical properties).

A comprehensive overview on computer-aided materials design for compound semiconductors based on pseudopotential methods, empirical interatomic potentials and computational methods at finite temperatures is given by [95Ito]. Predictions can be made for band structure, structural and thermodynamic properties. Applications are also exemplified for adatom migration and "bond engineering" [95Ito]. The problem of calculating the standard chemical potentials of electrons and holes in the case of degeneracy is also addressed by [89Sha] and applied to PbTe and SnTe semiconductors.

### 3.3 Interfacial reaction

The formation of interfacial reaction products during joining of different materials is an important factor that determines the joint properties. For example, in metal-ceramic joining or coating that has increased its importance for high temperature applications, the interfacial reaction products give significant effects on the mechanical properties of the metal/ceramic joints. The formation of intermetallic compounds during soldering is also closely related to the wettability of solder on the substrate as well as the reliability of soldering. Therefore, a detailed understanding and prediction of interfacial reaction would be helpful to alloy or process design in the joining process.

Potential diagrams have been widely used to predict or rationalize the interfacial reaction layer sequence, based on the idea [90Loo] that no element can intrinsically diffuse into a direction where its own chemical potential is increased. It is believed that potential diagrams can be used to find out whether a given interfacial reaction layer sequence is thermodynamically allowable or not, however can not give sufficient information for the reason why a certain layer sequence is formed during an interfacial reaction.

Recently, a new calculation scheme to predict the interfacial reaction product that forms first between different materials has been suggested [97Lee1, 97Lee2]. In that scheme, a local equilibrium is assumed at the phase interface before the formation of interfacial reaction products. The interface compositions are expected to be located somewhere on the metastable phase boundaries between the two phases, and can be determined from the tie-line. Generally, in a multicomponent system, there exist infinite number of tie-lines between two phases at a given temperature and pressure. The tie-line that corresponds to the thermodynamic state at the interface can be determined by a simulation for the multicomponent diffusional reaction between the two phases. Under the metastable local equilibrium state, the driving forces of formation for individual phases are calculated and the phase with the highest driving force of formation is selected as the first-forming interfacial reaction product between the initial phases. By repeating the application of the same scheme to the newly created interfaces between the newly formed phase and the initial phases, or by applying the scheme based on the potential diagram, the whole layer sequence can be predicted.

The application of the present scheme is confined to the case where a diffusion controlled reaction can be assumed. Further, for a complete prediction of the formation of interface reaction products, the nucleation activation energy for each phase should be compared. For the estimation of the nucleation energy barrier the interface energy and misfit strain energy, the information of which is lacking, should be considered, as well as the driving force. However, the driving force can be a good approximate criterion for prediction of the first-forming phase for high temperature interfacial reactions, where the portion of the interface energy and misfit strain energy in nucleation kinetics can be assumed as relatively small.

This scheme has been successfully applied to the prediction of the interfacial reaction between Cu substrate and various liquid solder alloys [97Lee1], and between pure titanium and alumina [97Lee2]. The results will be briefly presented here.

It is well known that the intermetallic compound that forms first between Cu substrate and Sn-Pb solder is $Cu_6Sn_5$ (for example, [93Via]). On the other hand, recently it has been reported that the first-forming phase between Cu and Sn-Zn solder is $\gamma$-$Cu_5Zn_8$ [97Yoo]. The reason for the difference in the first forming phase

during the two interfacial reactions can be explained by applying the present scheme in each reaction. According to the present scheme, a metastable equilibrium should be built up between the Cu substrate and the liquid solder. The interface composition of each phase is determined from the tie-line that corresponds to the thermodynamic state at the interface. Due to the relatively high diffusivity in the liquid, it can be assumed that the atomic ratios between solder components (Sn/Pb, or Sn/Zn) at the interface in liquid are the same as those of initial solder alloys. By this, the tie-line can be determined even without diffusion simulation. Under the metastable equilibrium state at the interface, $Cu_6Sn_5$ is calculated as the phase with the highest driving force of formation in the case of the Cu-Sn-Pb system, while in the Cu-Sn-Zn system $\gamma$-$Cu_5Zn_8$ is calculated as that phase. Therefore, it can be concluded that the difference in the first forming phase between each solder alloy originates from the difference in thermodynamic state at the interface, and such difference can be well predicted by calculating metastable phase equilibria between initial phases.

For the interfacial reaction between $\beta$Ti (bcc) and $Al_2O_3$ at 1100 °C, the same scheme can be applied. The difference from the above interfacial reactions (Cu/solder) is that the composition of the $\beta$Ti matrix phase at the interface can not be determined by only calculating the metastable phase boundary between the initial two phases. In order to estimate the interface composition of the $\beta$Ti matrix phase, a diffusion simulation can be performed as has been described in [97Lee2]. In Figure 3.3.1, the simulated diffusion paths (thick solid lines) after various reaction times at 1100 °C are represented together with the metastable phase boundary between the two phases (thin solid line) and stable phase boundaries (thin dotted lines) at the same temperature. It is shown that at the beginning of the interfacial reaction the interface composition of the $\beta$Ti matrix phase stays at about 46 at.% Al - 0.8 at.% O. At this composition, the phase with the highest driving force of formation is calculated as TiAl, which leads to a prediction that TiAl would form first during the interfacial reaction between Ti and $Al_2O_3$ at 1100 °C. The diffusion simulation (Figure 3.3.1) also shows that when the Ti layer is saturated with oxygen, (when the potential gradient of oxygen in the Ti layer almost disappeared), the oxygen potential level in the layer phases increases with increasing reaction time, while the stability of TiAl decreases and that of $Ti_3Al$ increases. Therefore, it can be expected that TiAl forms first between Ti and $Al_2O_3$, but is replaced by $Ti_3Al$ after the saturation of oxygen in the Ti layer. Such a saturation of oxygen in the Ti layer will happen quickly when the initial Ti layer is thin. In that case, TiAl may not be observed at the interface because the replacement of TiAl by $Ti_3Al$ will happen quickly before the observation. On the other hand, when the initial Ti layer is thick, the saturation of oxygen will take time and TiAl will be well observed. It should be noted that TiAl has been observed only when the initial Ti layer was relatively thick while $Ti_3Al$ has always been observed during the Ti/$Al_2O_3$ interfacial reactions [92Li, 92Zha].

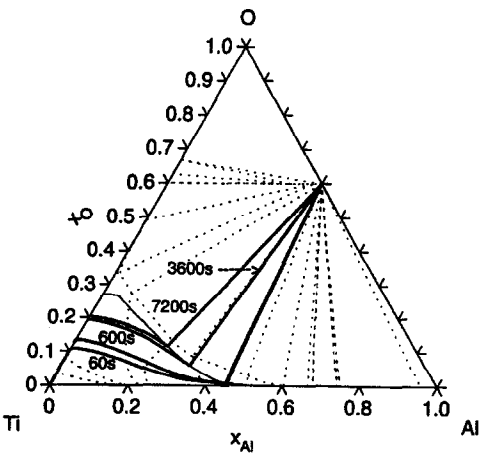


FIG. 3.3.1
Simulated diffusion paths (thick solid lines) between pure Ti and $Al_2O_3$ after various reaction times at 1100°C. Equilibrium isothermal section (thin dotted lines) and metastable phase boundary between $\beta$Ti and $Al_2O_3$ (thin solid line) are overlapped.

It has been shown that the driving force criterion can be successfully applied to metal/solder and metal/ceramics interfacial reactions. It is expected that the present scheme be applicable to interfacial reactions between wide range of materials, and contribute to rationalize the evolution of layer sequences.

### 3.4 Steelmaking processes

The strong competition in today's steel industry requires continued product development and process control and improvement as basic tools for survival. While the steel industry has been one of first materials industries to apply thermodynamics to improve the understanding of processes, further develop them and improve their control,

the complexity of the systems involved and the number of process variables have limited the contribution given by thermodynamics mostly to the indication of trends.

Several processes employed today have been developed more or less empirically and are currently controlled with statistical or experience-based models. More recently, thermodynamics has been used more often both in process and product development while its application in process control is still quite limited. The development of computational thermodynamics has made possible the treatment of complex systems that would previously require either excessive simplification or unreasonably complicated approximations.

In the following sections some examples of steelmaking problems that can be solved with the help of computational thermodynamics will be presented. Furthermore, the current limitations and foreseen improvements of these applications will be highlighted.

***Inclusion Control***

The control of non-metallic inclusions formed during steel processing is critical in defining its properties and processability.

Measures for the prevention of formation of solid inclusions that may clog continuous casting nozzles have been successfully modeled (*e.g.* [93Kub, 97Oer, 96Hac]). In this case it is apparent that the phases that influence nozzle clogging are close to equilibrium with steel, so that phase equilibrium calculation can be applied directly. Furthermore, as these phases precipitate from the liquid steel, this is the only Fe rich phase that must be considered. As an example of the results, Figure 3.4.1 shows recommended calculated compositions to guarantee the absence of solid phases at casting temperature, compared with experimental results. It has been well established that hard, undeformable inclusions (such as $Al_2O_3$) can be deleterious for processing and performance of several types of steels. One approach for preventing the formation of these inclusions has been the adjustment of the steel composition in a way that upon cooling from the liquid, no high melting point inclusions would precipitate. In the case of tire cord steels or valve spring steels, successful calculations have been performed using the conventional approach with direct data from phase diagrams (*e.g.* [96Sui]) and also via thermochemical modelling (*e.g.* [87Gay, 92Gat]). As the complexity of the slag and inclusions systems involved is evident, the advantages of computational thermodynamic techniques is clear [97Oer, 92Gat]. In this case, one can first define the range of inclusion compositions acceptable

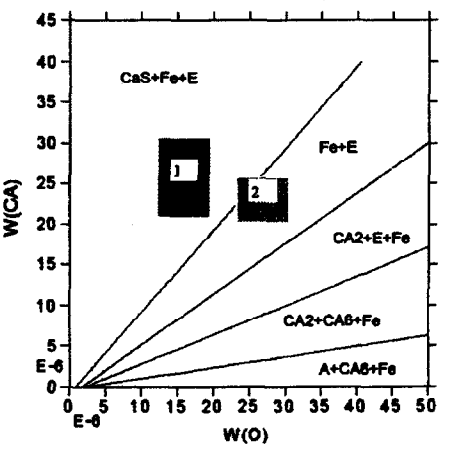


FIG. 3.4.1
Portion of the Ca-Fe-S-O diagram at 1600 °C (S = 50 ppm and Al = 0.04 %). Phases in equilibrium with liquid steel (aluminates CA2, CA6, $Al_2O_3$ (A) and liquid inclusions (E)) are indicated. Experimental results of Pellinani [86Pel]: Region 1: presence of CaS. Region 2: absence of CaS

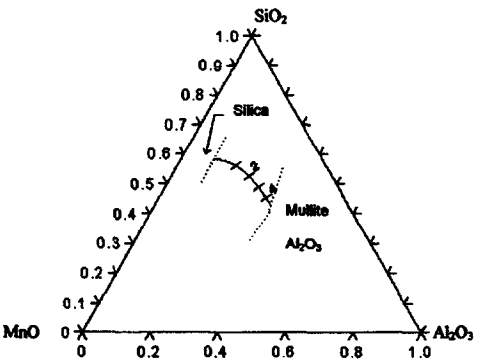


FIG. 3.4.2
1550 °C isotherm in the MnO-$SiO_2$-$Al_2O_3$ system. The solid line indicates the Al content (in weight ppm) of steel in equilibrium with liquid slag. (Steel contains C = 0.8 %, Mn = 0.6 %, Si = 0.3 %. Regions of solid precipitation are indicated.)

from the properties point of view and then the steel composition such that these will be the inclusions that precipitate upon cooling. This again assumes equilibrium precipitation, but apparently the results are satisfactory if it can be guaranteed that the inclusions formed will be in the low melting region. Figure 3.4.2 shows that, in the case of high carbon, silicon-manganese steels, there is a very narrow range of aluminum contents in the steel that will be compatible with the formation of low melting inclusions. With this information one can then design a slag for ladle furnace treatment that will guarantee the very low aluminum contents required. The evident advantage of the computational thermodynamics approach in this case is that the effect of all relevant solutes in the steel and in the slag can be taken properly into account, which is not always possible when doing calculations based on data tabulated or extracted directly from the available phase diagrams.

The desire to improve control over microstructure in current applications, as well as the need to consider how microstructure will be controlled with the emerging generation of near-net-shape continuous casting processes has lead to the concept of "oxide metallurgy" [89Ues, 94Ogi]. In this concept, the control of inclusion composition and distribution would play a paramount role in defining nucleation sites for austenite to ferrite transformation. In order to properly understand inclusion formation and distribution during solidification, a good knowledge of solute redistribution during solidification is also required (*e.g.* [86Ues, 96Miz]). (see also the section on Continuous Casting).

Currently the models available for slag description are simplified approximations [94Hal, 93Sel, 84Gay]. Hence, some important systems are very difficult to describe properly. Furthermore, there is not an established way of converting data among these models, which further complicates their use [97Hil]. It is necessary that thermodynamic software can handle different species in different phases for efficient slag metal equilibrium computations.

Data in some important slag systems are still missing. There is still controversy over the melting point of CaO, for instance, and no database has a good description of fluorine containing slags.

The vast majority of the inclusions that form in steel are either oxides or sulfides. While a liquid iron description derived from dilute solution data [74Sig, 86Hil] is available, the current CALPHAD assessments of the Fe-O and Fe-S systems use an ionic liquid model, which makes it difficult or impossible to combine these binaries with other relevant CALPHAD assessments such as Fe-Al, Fe-Si, etc. Another critical aspect is the fact that a large number of the applications in steelmaking presently require good knowledge of the behaviour of dilute solutions. Steel systems will benefit from better descriptions in the dilute range, even if, at the present state, this would somehow sacrifice the across-the-range description of the system. In the future, descriptions that are accurate enough both in the dilute and overall range will hopefully be achieved.

***Converter steelmaking***

Thermodynamics has been a part of converter steelmaking modelling since the introduction of the "static control" models [96Tur, 88Cos]. In order to achieve good control results, these models have frequently been coupled with statistical data in order to accommodate uncontrollable variables. The efficiency of these models in achieving ready to tap heats is, however, limited. The introduction of "dynamic control" with the use of sublance [96Tur, 91Nak] to improve the control of the last stages of decarburization has significantly improved the percentage of ready to tap heats. Most of these models, to date, are based on statistical parameters.

In order to better understand the processes occurring in the converter, several kinetic models have been proposed to describe hot metal conversion [*e.g.* [87Deo, 93Cho]). Most of these models assume that equilibrium prevails at the interfaces: they thus incorporate some sort of thermodynamic tool and transport kinetic model. Deo and co-workers [87Deo, 92Kno] for example, have used classical Wagner formalism to describe the behaviour of solutes in the liquid metal and incorporated a cell-model to describe the slag behaviour. The limitations of the use of simplified thermodynamic models in the prediction of slag behaviour and thus of the overall converter behaviour are well established [93Deo, 87Deo]. Figure 3.4.3 presents some of the results that can presently be obtained with these simple models [98Cas]. These results show general agreement with plant data and can be used to perform preliminary investigations on the effects of changes of converter practice, but are not sufficiently accurate to be developed into control tools.

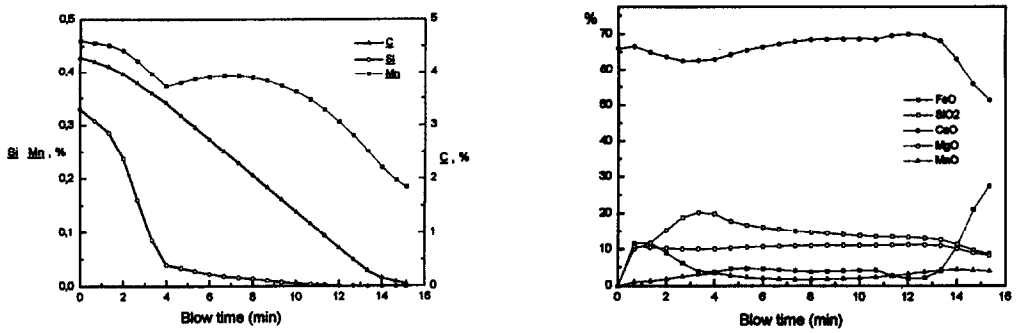


(a) (b)

FIG. 3.4.3
Calculated composition evolution of liquid metal and slag using a converter model that couples thermodynamics and kinetics [98Cas]. (a) Liquid metal composition. (b) Slag composition

With the availability of good software interfaces to connect kinetic models to thermodynamic equilibrium software, these results will probably improve significantly, although the uncertainties derived from the complexities of the fluid flow conditions in the converter will still limit their applications as control tools.

***Slag-refractories interactions***

Commercial software packages that predict how to prevent slag aggression to refractories are presently available, mostly from refractory manufacturers. Most of these software packages are based on empirical relations to predict slag saturation in the relevant phases present in the refractory. In this case too, an easy interface with a thermodynamic equilibrium calculation software will improve the ability of these software to predict the most adequate slag compositions from the point of view of compatibility with refractories.

***Continuous casting***

Extensive modelling work has been performed to predict thermal evolution and fluid flow conditions in continuous casting, and have been review elsewhere (*e.g.* [95Bri, 95Tho]). In order to understand segregation and inclusion precipitation at the currently required level, however, models that incorporate solute redistribution have been developed. Several models that describe dendritic segregation have been developed and tested [86Ues, 92Mat, 95Ohs, 95Mat] (see also reviews [92Bat, 95Ste]). In most cases, empirical relationships between liquidus temperatures and compositions as well as effective or averaged partition coefficients have been used in these models. Under these conditions the coupling of the thermal model and the metallurgical evolution of the microstructure is somewhat limited.

With the development of interfaces for the computational thermodynamic software, it is now possible to provide equilibrium interface compositions and enthalpy contents to the thermal/ fluid flow models. It is expected that this will then make possible to incorporate better predictions of segregation, inclusion formation and carbonitride precipitation in the current thermal/ fluid flow models. An specific example is discussed in the Solidification section of this report.

***Overall Recommendations***

It is evident that a large segment of new applications of computational thermodynamics in steelmaking can derive from the coupling of thermodynamic calculations with kinetic models; furthermore, a segment of emerging applications will become viable if some improvements in the current computational thermodynamic toolbox are made.

It is suggested that the following actions will facilitate the development of these new and emerging applications:

a) Easy interfacing between thermodynamic calculations software and codes written by users or commercial software should be available. At this point one interface (TQ) has been offered and is being tested in several applications.
b) Develop methods for evaluating and predicting the transport properties needed to describe the dynamic state of phases. These properties may include molecular diffusivities, viscosities, thermal conductivities. One must recognize the different formulations of the equations of change used amongst different researchers. Whether this will evolve from the present computational thermodynamic community or not, is still a point of debate.
c) Steel, aluminum alloys and several complex commercial systems will benefit from better descriptions in the dilute range, even if, at the present state, this would somehow sacrifice the across-the-range description of the system. In the future, descriptions that are accurate enough both in the dilute and overall range will hopefully be achieved.
d) Models for slags that can treat easily the formation of non-metallic inclusions in steels and superalloys (for instance) and have high compatibility with the usual models employed for liquids in the CALPHAD approach, would be useful. Furthermore, thermodynamic equilibrium software that is able to treat, in the same problem, different species in different phases would greatly simplify the work of those applying them to slag-metal or inclusion-metal equilibria.

### 3.5 Solidification

The coupling of macroscopic and microscopic models is important for the accurate description of the casting process and the resulting microstructure [88Rap, 89Rap]. Macroscopic modelling involves heat and fluid flow in the casting, whereas microscopic modelling is necessary for the analysis of the variation of liquid and solid concentrations during cooling through the "mushy" temperature regime. The two are coupled through the details of the latent heat release. Kraft and Chang [97Kra] recently presented an overview of the various methods which were developed for microscopic modelling during the past 30 years. They also give an extensive list of examples of the increasing number of solidification simulations that are coupled with phase equilibria calculation for multicomponent alloys.

Although many solidification micromodels have been developed for binary alloys, commercial alloys generally require the consideration of three or more components. Thermodynamic modelling of multicomponent phase diagrams using the CALPHAD method has been shown to be a successful method to limit the amount of experimental effort required to treat the constantly growing list of commercial alloys [94Sau]. The level of complexity of micromodels vary considerably, but all require phase diagram information such as the concentrations at the liquid-solid interface, the liquidus slopes and the partition coefficients which can be obatined from phase equilibria calculation. Even though phase diagrams represent thermodynamic equilibrium, it is well established that the phase diagram can be applied locally (local equilibrium) to describe the solidification path where only the concentrations at the liquid-solid interface are assumed to obey the requirements of thermodynamic equilibrium. However, in some instances corrections may be needed. In the following results of calculations from Boettinger *et al.* [95Boe], Kattner *et al.* [96Kat], Banerjee *et al.* [97Ban] and Schneider *et al.* [97Sch] are presented as examples.

#### *Simple solidification calculations*

Two simple models describe the limiting cases of solidification behaviour. For solidification obeying the lever rule at each temperature during cooling, complete diffusion is assumed in the solid as well as in the liquid, thus all phases are assumed to be in thermodynamic equilibrium during each temperature during solidification. In comparison, solidification following the Scheil path where diffusion in the solid is forbidden produces the worst case of microsegregation with the lowest final freezing temperature. Thermodynamic equilibrium exists only as local equilibrium at the liquid/solid interface. Calculations for these two limiting cases of solidification behaviour were carried out by Boettinger *et al.* [95Boe] and are shown for an IN718 alloy (initial composition: 52 wt.% Ni, 19 wt.% Cr, 0.25 wt.% Co, 0.9 wt.% Ti, 0.02 wt.% Ta, 0.55 wt.% Al, 3.05 wt.% Mo, 4.85 wt.% Nb and 19.4 wt.% Fe) in Figure 3.5.1. The final microstructure from the Scheil solidification is predicted to contain 0.018 fraction of Laves phase, while for the unlikely case where complete diffusion is present in the solid as well as the liquid (lever rule solidification) no Laves phase formation was predicted. Thus, Laves phase in cast IN718 is predicted to be a "non-equilibrium" phase in the sense that long term annealing removes it from the cast structure,

as confirmed by [91Cao]. Modelling of real solidification behaviour requires the incorporation of a kinetic analysis of microsegregation and back diffusion.

***Back diffusion analysis***

Boettinger *et al.* [95Boe] also carried out a solid diffusion calculation for the primary phase of IN718 during solidification, retaining the assumption of a completely mixed liquid. In the limits of zero and infinite amounts of solid diffusion, these calculations recovered the Scheil and lever results described above. During eutectic solidification, solid diffusion was neglected.

The diffusion analysis revealed that for usual cooling rates and experimentally observed secondary arm spacings [95For], the solidification path for IN718 deviated only slightly from the Scheil results. The $T(f_s)$ result for 0.1 °C/s is shown in Figure 3.5.1. Similar behaviour was found by Meurer *et al.* [97Meu] for a commercial aluminum alloy. Due to the high diffusivity of carbon Meurer *et al.* found that for the solidification of steels that the effect of back diffusion resulted in fraction solid vs. temperature curves which were close to those obtained from the lever calculation.

***Dendrite tip analysis***

In the previous examples, transport of solute in the liquid phase was assumed to be sufficiently rapid that the liquid could be assumed to be uniform in concentration during cooling. Whereas this provides an excellent first approximation to the solidification path, two factors can lead to a lowering of the temperature where solidification first begins: nucleation and the lack of a uniform liquid due to finite diffusion rates. Kattner *et al.* [96Kat] also give an example for the latter.

Figure 3.5.2 shows the dendrite tip velocity and tip radius versus tip temperature for the IN718 alloy. For zero temperature gradient, the dendrite tip temperature approaches the liquidus temperature if the dendrite tip velocity approaches zero. With increasing dendrite tip velocity, the dendrite tip temperature drops below the liquidus. Thus the first solid forms at a temperature below the liquidus. A non-zero value of the temperature gradient causes the curves to turn at low velocity. This effect is due to the approach to the conditions that would lead to plane front solidification by avoiding constitutional supercooling/morphological stability. The effect of the temperature gradient is small for practical values of speed present in castings.

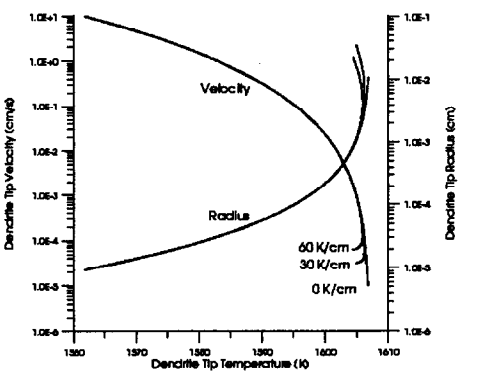


FIG. 3.5.2
Dendrite tip velocity and tip radius vs. temperature computed for IN718 for three values of the liquid temperature gradient

The results for zero temperature gradient are customarily applied to the simulation of equi-axed castings and in the cellular automaton simulations, *e.g.* Gandin and Rappaz [94Gan].

***Coupling of Dendrite Analysis to the Subsequent Solidification Path***

Coupling of the dendrite tip analysis to the description of the solidification path at temperatures below the dendrite tip temperature have been performed for binary alloys by Rappaz and Thévoz [87Rap] and has been applied to equi-axed castings and by Giovanola and Kurz [90Gio] for rapid solidification. The former approach also permits the inclusion of undercooling due to the details of nucleation and the computation of recalescence or reheating due to rapid dendritic growth. Frequently, however, a simpler approach is used to couple the dendrite tip analysis to the remainder of the solidification path.

Grafe at al. [98Gra] coupled a dendrite tip analysis and Scheil solidification calculation with a pseudo 2-dimensional model of dendrite growth. The concentration profiles were calculated for a CMSX4 alloy and compared with EDX measurements of a directionally solidified sample. The calculation predicted qualitatively the segregation behaviour.

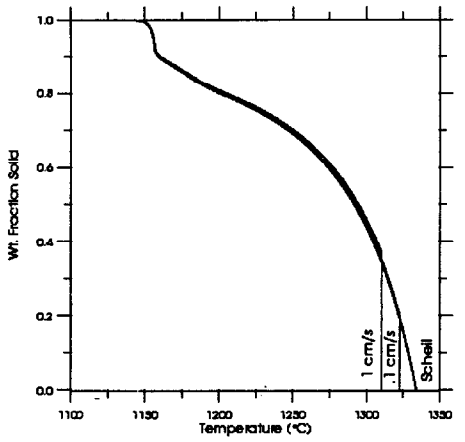


FIG. 3.5.3
Calculated fraction solid vs. temperature curves for IN718 for two growth speeds that combine the dendrite tip analysis with a Scheil model for the subsequent freezing at lower temperatures.

The "truncated Scheil" method was proposed by Flood and Hunt [87Flo] for binary alloys. With this method the fraction solid versus temperature curve is developed by merely assuming that during cooling the fraction of solid jumps from zero to the value given by the standard Scheil analysis at the temperature at which the dendrite tip is operating. This approach is extremely attractive for its simplicity and has been employed by Gandin and Rappaz [94Gan] in their cellular automata research. A difficulty with this approach is that solute is not conserved. Kattner *et al.* [96Kat] corrected this deficiency by an alternate procedure that is only slightly more complicated but does require modelling the remaining solidification path differently at each node of a macroscopic heat flow model. This procedure also permits extension to multicomponent alloys. The result of such an analysis for IN718 is shown in Figure 3.5.3. With this approach the effect of dendrite tip kinetics on the variations in fractions of second phases can be determined. For the alloy shown, however, it is apparent that the "truncated Scheil" approach would have been an excellent approximation for the indicated growth speeds.

***Solidification micromodel and FEM coupling***

A procedure for coupling thermodynamic calculation of phase equilibria parameters with a micromodel for computing the fraction solid and temperature change for a specific enthalpy change during the liquid solid

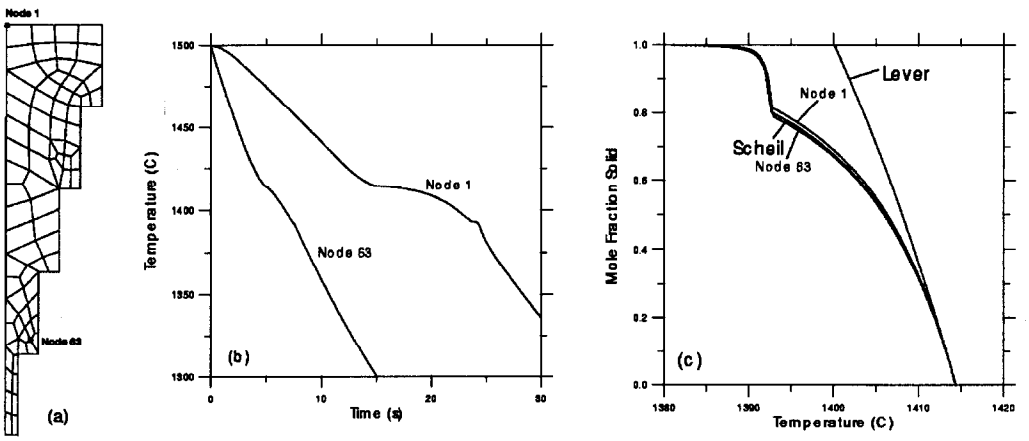


FIG. 3.5.4
(a) FEM mesh and location of selected nodes. (b) Temperature vs. time from the simulations. (c) Fraction solid vs. temperature.

transformation and its implementation into a finite element package for modelling the solidification of castings has been presented by Banerjee *et al.* [97Ban].

Fully coupled FEM simulations were performed on a step wedge part with 105 nodes for a Ni - 15 at. %Al - 2 at.% Ta alloy. Figure 3.5.4 (a) shows the right half of the symmetric part and two nodes of interest (node 1 and 63). The different cooling histories revealed by these two nodes are shown in Figure 3.5.4 (b). The fraction solid-temperature curves were generated during the run-time of the macroscopic model and thus depend on the actual cooling histories shown in Figure 3.5.4 (b). The curves for the two nodes are shown in Figure 3.5.4 (c). The fraction solid- temperature curves from a Scheil and lever rule calculation are also shown in Figure 3.5.4 (c). The curve for the slower cooling node (node 1) lies above that for the fast cooling node (node 63), *i.e.* towards the prediction of equilibrium solidification from the lever rule.

***Mushy zone simulations***

Schneider *et al.* [97Sch] numerically simulated the formation of macrosegregation and freckles by multicomponent thermosolutal convection during the directional solidification of single crystal Ni-base superalloys. For their simulations, thermodynamic phase equilibrium code was linked with code for finite difference convection calculations. The calculations were carried out in a fully coupled manner, simultaneously solving macroscopic mass, momentum, energy and species conservation equations for the solidification of a multicomponent alloy.

The simulations revealed that the onset of convection coincided with the occurrence of channels and freckle defects and depends primarily on the primary dendrite arm spacing which is a consequence of the imposed cooling rate. For a CMSX2 alloy it was found that the critical primary dendrite arm spacing for the onset of convection is in good agreement with experimentally observed values. Even though the results from these two-dimensional simulations were in agreement with experimental observations, Schneider *et al.* noted that freckling is inherently a three-dimensional problem. Although Schneider *et al.* encountered no major problems in linking the phase equilibrium code to the solidification code, computational times increased excessively and special procedures had to be used to limit the number of calls to the phase equilibrium subroutine.

In order to use this kind of calculations in a fully coupled manner for the simulation of industrial processes, a reduction in computation time is imperative.

### 3.6 High-performance coatings

The increasing importance of coatings produced by PVD (physical vapour deposition) techniques for wear and corrosion resistance applications is leading to the systematic development of new high-performance coating materials. Because the adhesion and oxidation resistance of classic thin films such as TiN, TiC and $Al_2O_3$ are not always adequate, experiments with the deposition of metastable, multicomponent coatings are being carried out. Using PVD methods, it is possible to achieve required coating compositions relatively easily. By varying the substrate temperature, it is sometimes possible to change the structure of the deposited material. The properties of the coating are thereby changed.

By carrying out thermodynamic calculations, it is possible to predict the conditions for the appearance of possible metastable phases during PVD coating processes and thereby assist in the selection of coating parameters required to produce coatings with optimum desired properties.

The general principle relating to thermodynamic calculation of the metastable phase ranges resulting from PVD of multicomponent coatings on a low-temperature substrate has been propounded by Saunders and Miodownik [86Sau] as follows:
"If an alloy that in equilibrium contains a multiphase structure is co-deposited at low enough temperatures, the surface mobility is insufficient for the breakdown of the initially fully intermixed depositing atoms, and the film is therefore constrained to be a single-phase structure.....Nucleation and subsequent growth processes are controlled by the substrate temperature, and therefore, if the film is constrained to be a single phase, the structure of the film should reflect the most energetically stable single-phase form available to it at the temperature of the

substrate. This phase can be directly found from the Gibbs energy versus composition (G/x) diagrams of the alloy system of interest..."

Making use of the above principle a series of calculations has been made for various possible coating combinations from among the constituents TiN, TiC, ZrN and HfN (all with the cubic NaCl structure) with AlN or SiC (hexagonal wurtzite structure) or $TiB_2$ (hexagonal structure) [90Spe, 93Sto]. Additional calculations have been carried out for coatings in the $Al_2O_3$-AlN system [98Spe].

*(Ti,Al)N coatings*

The important potential of thermodynamic calculations in predicting the ranges of composition and temperature in which different metastable phases may form in a particular coating system is exemplified by calculations for TiN-AlN coating combinations. Metastable (Ti,Al)N coatings with the cubic NaCl structure are already being produced commercially for cutting tool applications. They have been shown to exhibit superior performance as compared to TiN under conditions of wear at elevated temperatures due to their better oxidation resistance and hardness. The oxidation resistance of the coatings increases significantly with increasing Al-content. However, the deposition of (Ti,Al)N films with Ti/Al ratios below about 30/70 leads to a hexagonal coating structure which is not suitable for tribological coatings. Relatively little is known about the location of the cubic to hexagonal phase transition and hence about the optimum composition of (Ti,Al)N hard coatings.

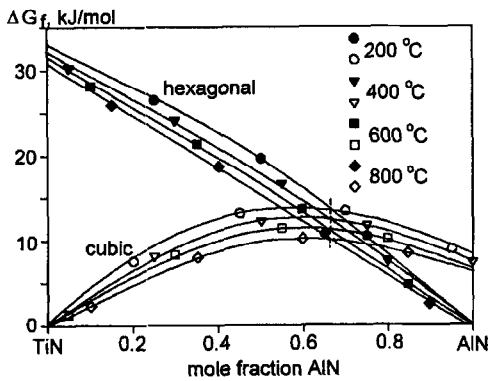


FIG. 3.6.1

Gibbs energy of formation of the hexagonal and cubic phases for AlN-TiN system as a function of composition at 200, 400, 600 and 800 °C.

From a thermodynamic analysis of the Ti-Al-N system, involving estimation of Gibbs energy differences between cubic NaCl and hexagonal, wurtzite structural forms of TiN and AlN, Gibbs energy curves were calculated for the hexagonal and cubic phases for various temperatures in the section AlN-TiN (Figure 3.6.1). The point of intersection of these curves at each temperature defines the composition at which there is a transition from one structure to the other. These curves are also called $T_0$ cureves. It can be seen that this composition is nearly temperature independent and has a value close to 0.69 mole fraction AlN.

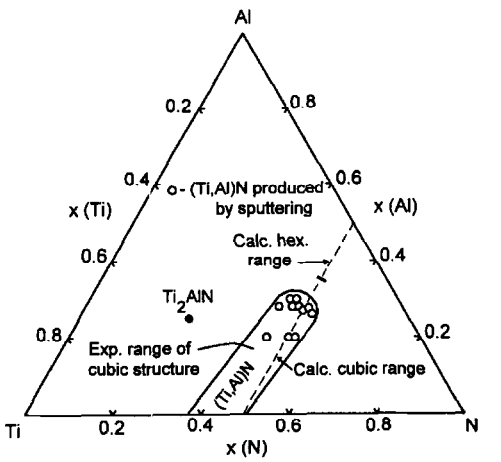


FIG. 3.6.2

Comparison of experimental [87Kno] and calculated range of the metastable NaCl cubic structure in the section AlN-TiN.

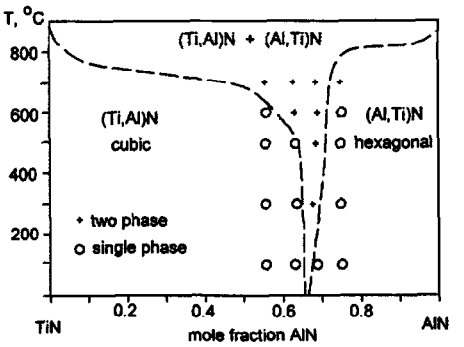


FIG. 3.6.3

Modified metastable (Ti,Al)N phase diagram according to the experiments performed in the work of [98Cre].

Experimental studies of the approximate extent of the metastable cubic range in the section AlN-TiN have been carried out by Knotek and Leyendecker [87Kno] (see Figure 3.6.2) and more recently, with greater accuracy, by Cremer *et al.* [98Cre] using electron probe microanalysis, X-ray photoelectron spectroscopy and thin film X-ray diffraction. The latter study showed that for co-deposition temperatures between 300 and 700 °C, a two-phase region exists in the metastable AlN-TiN phase diagram. This expands with increasing temperature, whereas at 100 °C substrate temperature, no two-phase region was observed (Figure 3.6.3). The composition of the structural transition in the experimental studies lies between about 0.63 and 0.69 mole fraction AlN. The calculated transformation composition is therefore in good agreement with these observations.

Based on the experimental work, new $Ti_{1-x}Al_xN$ hard coatings for tribological applications with a composition 0.62 mole fraction AlN has been developed, which shows an increase of oxidation resistance by a factor 4 over conventional TiN coatings.

### *$TiB_2$-TiC coatings*

Similar calculations to those described above have been carried out for coatings corresponding to compositions in the section $TiB_2$-TiC of the Ti-B-C system [90Spe]. Using evaluated and estimated Gibbs energy data based on available phase diagram information, the Gibbs energy curves for the section $TiB_2$-TiC were calculated for a temperature of 500 K. These are shown in Figure 3.6.4 together with the experimentally observed structures at selected compositions. There is excellent accord between the calculated and experimental results.

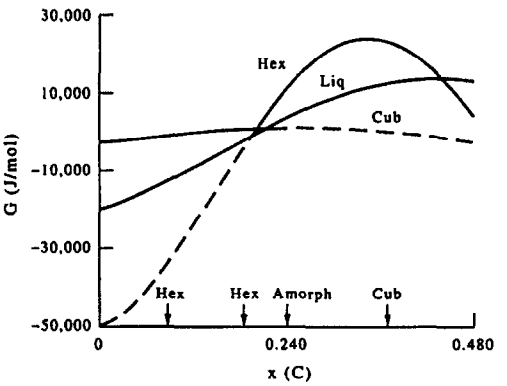


FIG. 3.6.4
Calculated Gibbs energy curves for the cubic, hexagonal and liquid phases of the Ti-B-C system in the section $TiB_2$-TiC at 500 K.

### *$Al_2O_3$-AlN coatings*

The combination of the advanced physical properties of the electrovalent $Al_2O_3$ with the covalent AlN, which in equilibrium show no reciprocal solubility in the solid state at temperatures < 1627 K [92Hil], in the form of a metastable, homogeneous phase consisting of all three elements Al, O and N, could be of considerable technical interest. The refractive index of a pure AlN film is high [88Wan], the refractive index of $Al_2O_3$ is low [87Wan], the thermal conductivity of AlN [86Smi] is high compared to that of $Al_2O_3$ [88Sch]; AlN is a semiconductor, $Al_2O_3$ an insulator. Supposing the homogeneous metastable Al-O-N phases with variable composition can be stabilized by vapour deposition due to low adatom mobilities, then perhaps the different properties of the binary compounds can be combined.

Metastable Al-O-N layers have been produced by reactive magnetron sputtering ion plating using an Al target and an Ar-$O_2$-$N_2$ gas mixture [96Ric]. At 190 °C substrate temperature and variable partial pressures of $O_2$ and $N_2$, a variety of coatings with different O and N contents were prepared and analysed by means of X-ray photoelectron spectroscopy, Auger electron spectroscopy, high-resolution transmission electron microscopy and high-resolution scanning electron microscopy. Oxygen-rich Al-O-N phases were found to be nanocrystalline with a cubic structure like gamma-$Al_2O_3$ (spinel), nitrogen-rich phases displayed a

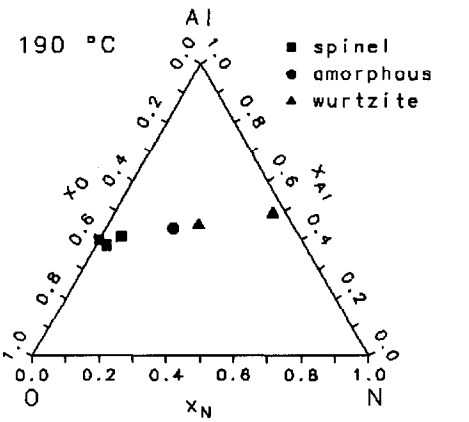


FIG. 3.6.5
Crystal structure of the phases observed in the metastable Al-O-N system.

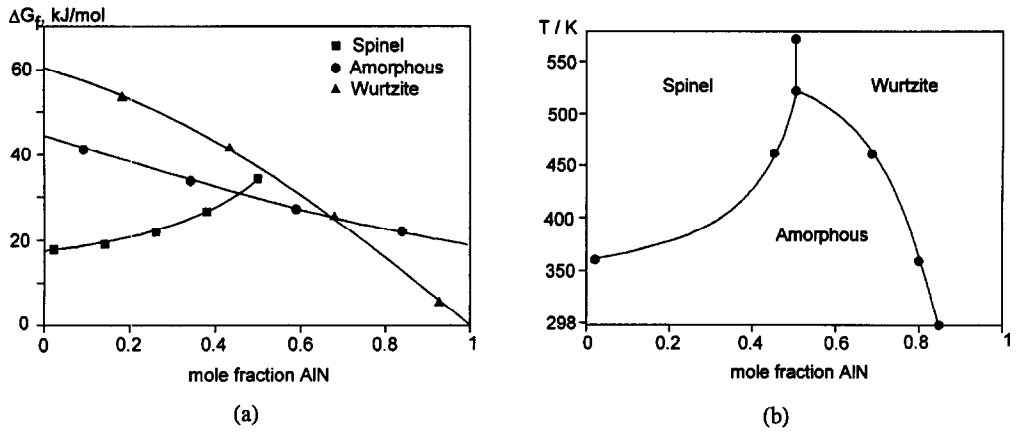


FIG. 3.6.6
(a) Gibbs energy of formation of stable and metastable phases in the $Al_2O_3$-AlN system at T=463 K. (b) Metastable phase regions in the $Al_2O_3$-AlN system.

hexagonal structure like AlN (wurtzite). Around O/N=1.5, the deposited phase was TEM amorphous (Figure 3.6.5).

Using Gibbs energy values provided by a thermodynamic evaluation of the $Al_2O_3$-AlN system [92Hil], and incorporating thermodynamic descriptions for the wurtzite and amorphous phases for the entire composition range, Gibbs energy curves as a function of composition have been calculated for the spinel, wurtzite and amorphous phases for temperatures between room temperature and 600 K. The curves for the deposition temperature used in the experimental studies are illustrated in Figure 3.6.6 (a), and from the *loci* of the points of intersection of these curves as a function of temperature ($T_0$ curves) the deposition ranges of the phases have been determined (Figure 3.6.6 (b)).

The above examples illustrate that thermodynamic calculations are able to provide information of significant practical importance on the composition and temperature ranges of metastable coating phases and offer important predictive support in the development of new, multicomponent coatings with desired structures.

## 3.7 Light Alloys

### *Introductory Remarks*

Light metal alloys are used for a wide range of applications involving both wrought and casting alloys, for aerospace engineering, structural equipment, titanium aluminides for turbo-jet engines, aluminium-lithium based alloys, metal-matrix composites and high-strength low-density alloys for transport (automotives, lorries, trains), marine engineering, packaging and canning - universal beverage cans (UBC's) and for quite specific purposes *e.g.* litho plate. Applications extend to joining (solders, brazing, welding), waste processing and recycling, and materials handling and compatibility. For these applications a variety of mechanical and physical properties are required, and the properties of alloys are in part dependent on their phase constitution under specific environmental conditions. A knowledge of the phase constitution is therefore fundamental to the development of new and improved alloys, to their manufacture into marketable products and their end usage.

Commercial alloys contain many alloying elements, typically up to 8 or 10, some as alloying additions, some as residual impurities, making the possible variations in phase constitution almost infinite. Published phase equilibrium data for higher-order systems are scarce, and the experimental investigation of complex alloys is very

expensive and time-consuming, hence the reason for the calculational approach. The benefits of calculations include cost and time saving, process prediction, improved control of processes and corrosion control.

***Data Availability***

Although there are a number of thorough reviews of phase diagram data for light alloys *e.g.* for aluminium alloys [59Phi], [61Phi], [76Mon], [86Bak], [90Bak], for magnesium alloys [88Nay], for titanium alloys [87Mur], and general, [90Pet], [95Vil], it became evident some years ago that, unlike the situation for steels, a general paucity of reliable thermodynamic data, particularly critically assessed data in the form required for multicomponent calculations, exists for light metal alloys. Thus began in 1989 the European COST 507 Project which involved collaboration between research organisations from 14 counties [94Ans], [98Ans], [98Cha]. A thermochemical database for light metal alloys resulted from this (now completed) project containing datasets for 80 binary and 25 ternary systems [98Ans], together with many critical assessments of phase diagram information and results of experimental studies including thermo-physical data.

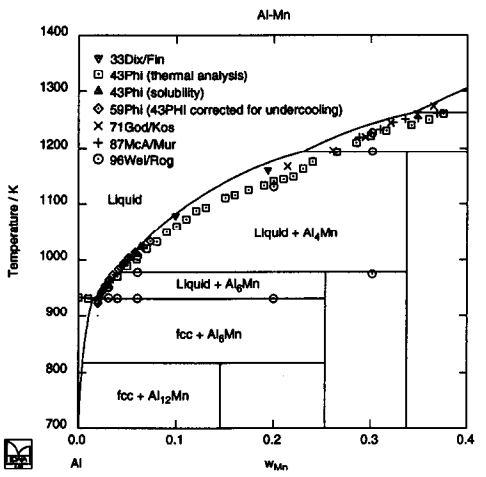


FIG. 3.7.1
Calculated partial phase diagram for the Al-Mn system, showing experimental data

The project did, however, show up some basic, unexpected problems in the published scientific literature. Namely undercooling (sometimes significant) of liquidus temperatures, see *e.g.* [98Ran], due in part to impurities, and also metastability. Figure 3.7.1 shows a calculated phase diagram for the Al-Mn system, with experimental data superimposed. The thermodynamic data employed, which form the basis for multicomponent calculations, have been computer optimised to take into account the experimental phase equilibria shown, and also the experimental thermodynamic properties.

The phase diagram data for this binary system, crucial to calculations for light alloys, has caused great concern due to experimental inadequacies. This assessment, [98Jan] is a modified and improved version of that in the original COST 507 database [92Jan], [94Ans] and represents a very satisfactory outcome according to current knowledge. Much painstaking work and careful analyses of the available information has been carried out by workers in the field. The experimental data, particularly for equilibria involving $Al_4Mn$, are fraught with problems due to the appearance of metastable phases, rather than the stable phase. This leads to low, non-equilibrium liquidus temperatures, which, however, are consistently reproduced by different experimental studies. For light alloys the most important part of the system is the range 0 to 4 or 6 wt % Mn, although for multicomponent calculations it is important to have a good overall representation of the system. The diagram shows the undercooling effects observed over the composition range 10 - 30 wt % Mn, almost certainly due to the appearance of metastable phases. Similar problems persist with data for *e.g.* the Al-Fe-Mn [98Jan] and Al-Mn-Si [98Ran] ternary systems.

***Applications***

Figure 3.7.2 (a) shows a calculated partial isothermal section for the Al-Si-Zn system at 825 K, giving details of the Al-rich corner, and Figure 3.7.2 (b) shows the calculated liquidus projection for part of the composition range. Although only for a ternary system, a combination of such diagrams have provided detailed information on the melting/solidification temperatures, crystallisation paths and the compositions of phases stable at different temperatures. This has been successfully used to assist the development of brazing technology for aluminium based alloy heat exchangers for automobile applications.

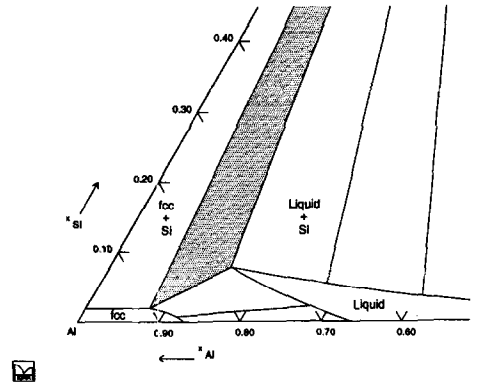


(a)

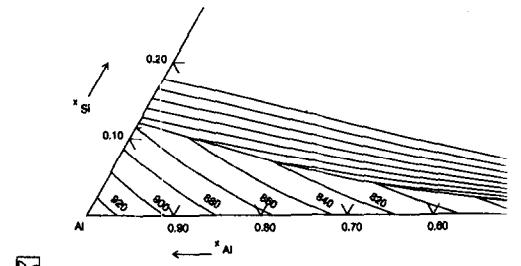


(b)

FIG. 3.7.2
Calculated partial isothermal section for the Al-Si-Zn system at 825 K and calculated liquidus projection for the Al-rich corner

Even relatively simple aluminium based alloys are surprisingly complex, and the types and amounts of phases present as precipitates can vary widely as a function of allowable composition variation within the specification. These variations can lead to extremely deleterious results, affecting, for example, surface quality of foil, and sheet for special purposes, and require control. The senary system Al-Cu-Fe-Mg-Mn-Si is important to the aluminium industry since it (or even some of the sub-systems) encompasses, *eg*, the 1000, 3000 and 5000 series wrought alloys. These cover major products including litho sheet, UBC body and can end material, and material for automotive applications (body panels, space frames etc).

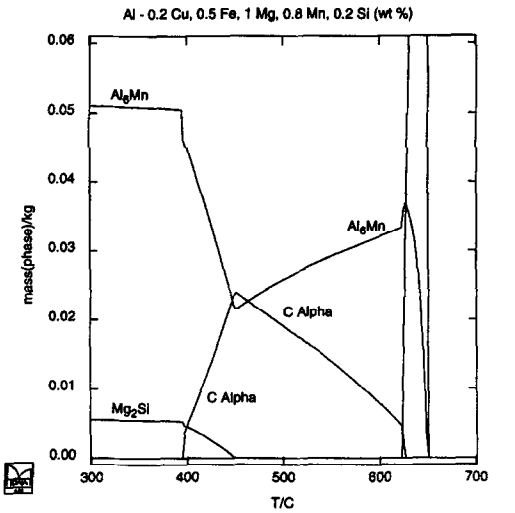


FIG. 3.7.3
Calculated mass fraction plot for an "idealised" 6 component 5000 series type alloy, showing the proportions of the phases present as a function of temperature. The plot is expanded to show more clearly the phases present. The main phase, when solid, is fcc.

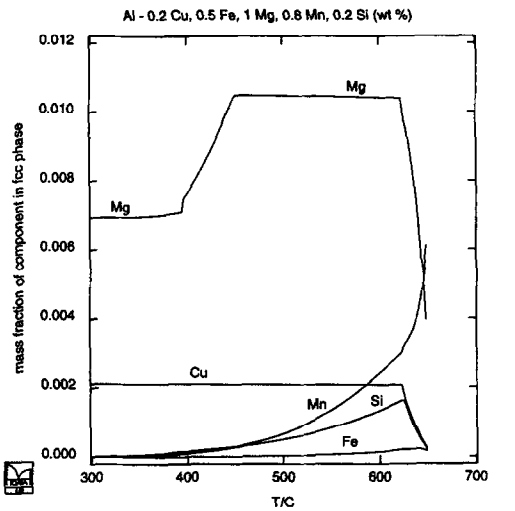


FIG. 3.7.4
Calculated mass fraction plot for an "idealised" 6 component 5000 series type alloy, showing the distribution of the components in the fcc phase.

Figure 3.7.3 shows a mass fraction plot for an "idealised" 6 component 5000 series type alloy containing Cu, Fe, Mg, Mn and Si, and indicates the proportions of the phases present as a function of temperature. The plot is expanded to show more clearly the phases present. The main phase, when solid, is fcc. The precipitation of

intermetallic compounds on cooling are quantified and the amounts of liquid and fcc are given. Figure 3.7.4 shows the distribution of the component elements in the fcc phase. Diagrams of this type are being used for many of the applications listed below. To determine such information by experiment, whilst crucial in specific test cases, would be prohibitively expensive and time-consuming. Such information is not only of relevance to the development and improvement of the above mentioned products, but also to their recycling. In this example data for the important cubic alpha AlMnSi phase are given.

Applications include:

- Design of model alloys to test accurately theories of microstructural evolution during thermo-mechanical processing:
  - with pre-defined phase(s) - coarse and dispersed
  - with pre-defined solute contents

- Prediction of cast microstructures:
  - liquidus temperatures as a function of solute
  - stable and metastable phase field location
  - composition dependence of partition coefficients

- Modelling of homogenisation processes:
  - solute controlled by nucleation and growth of dispersed phases
  - thermochemical data provides local boundary conditions

- The development of:
  - space frames and body panels, *e.g.* 5000 and 6000 series alloys, and for the development of high-strength fracture-tough alloys used to contain fuel for natural gas propelled vehicles - natural gas gives the lowest emission of carbon-based fuels.
  - piston alloys, which have quite different compositions from wrought alloys, often being hyper-eutectic with respect to the Al-Si system, ie 13-16 wt% Si and with additions of Ni. For this application grain-refining using *e.g.* TiC or TiB becomes important.
  - most users of alloys require, eventually, recycling technology, to remove *e.g.* Fe from the scrap, which is cheaper than smelter material. Recycling is equally important to transport applications as to packaging material.

***Examples of Success***

Two examples of the application of thermochemical data for light alloys, here from the COST 507 database, may be given, applicable to aluminium alloy design and optimisation, and efforts to improve recyclability of scrap, and to the development of titanium aluminide technology for high pressure compressor vanes for advanced gas turbines:

- "The COST 507 database for aluminium alloys has been widely used in model alloy work: knowledge of equilibrium conditions is a prerequisite for kinetic analyses of solidification, homogenisation and annealing. The final quinary database will be an invaluable tool for the European aluminium industry, applicable to alloy design and optimisation, process modelling and efforts to improve recyclability through increasing iron and silicon tolerance."
  Dr P V Evans, Alcan International Ltd, Banbury Laboratory
- "Titanium aluminides based on the TiAl phase are a relatively new class of lightweight high temperature materials that will find application in the gas turbine in the near future. The 1st generation alloys were based on Ti - 48 at% Al with additions of 2 - 4 at% transition metals. However the alloy chemistry was not optimised for gas turbine applications and the chemistry microstructure relationships were poorly understood. The titanium aluminide data from COST 507 has been used and extended by Rolls-Royce to assist in solving and understanding these problems. This has enabled a viable production process for small components to be identified and initial production for testing in advanced engine demonstrators is underway".
  Rolls-Royce plc

***Data Requirements***

Generally speaking, for aluminium-rich alloys, basic phase diagram data from the "scientific point-of-view" is well covered in the literature, although there are problem areas due to the complexity of the phase equilibria. There is, however, a lack of reliable data for some key phases from the industrial point-of-view. Most importantly, there is a lack of thermodynamic information for a great many ternary and higher-order systems:

- Phase diagram data:
  solubility of addition elements (*e.g.* Cr, Cu, Ti, Zn) in key phases - cubic alpha AlMnSi, hexagonal alpha AlFeSi and beta AlFeSi

- Thermodynamic data:
  stabilities (enthalpy, entropy) for many ternary compounds in the basic Al-Cu-Fe-Mg-Mn-Si-Zn system, many of which have large ranges of homogeneity

- Process modelling (see Section 3.5):
  need for new area of data - there is the requirement of data for solute-rich regions, currently much of the Al-database material pertains to relatively dilute alloys
  diffusion, mobility data

### 3.8 Hard metals

Hard metals consist of hard constituent grains bonded by a metallic phase. The hard constituent is often tungsten carbide and/or a cubic carbonitride phase based on for example Ti, Ta, Nb and W. The metallic binder is based on mixtures of Co, Ni and Fe. The hard constituents provide the hardness of the material and the metallic binder results in a much higher toughness compared to pure carbides or nitrides. This type of material has a considerable hardness up to temperatures of about 1100 °C. The main applications are chip forming machining of metals, rock drilling and wear parts.

The material is produced by mixing and wet milling of raw material powders with a grain size of the order of 1 μm. The milled slurry is mixed with an organic binder and spray dried resulting in agglomerates with a size of about 100 μm. The agglomerated powder is formed into products by uni axial pressing or injection moulding and consolidated by liquid phase sintering.

The compaction into complex geometrical shapes will result in a density distribution within the green body. The build up of the density distribution can be simulated by combining a commercial FEM code with a semi empirical model for the elastoplastic properties of the agglomerated powder [98Bra1]. The density distribution within the green body will result in a variation of sintering rates. The original density distribution will, thus, result in a change of shape of the sintered product. In order to control the change of shape a model for the sintering rate based on kinetic factors, material stiffness and thermodynamic properties has been developed. By implementing the model for the compaction and sintering into the FEM code it is possible to predict the density distribution after pressing and the shape of the product after sintering [98Bra2]. The predicted shape after sintering is in close agreement with experimental determination.

The hard metal products are often coated with multiple layers of hard coatings such as TiN, TiC and $Al_2O_3$ in order to increase the hardness, the abrasive wear resistance and decrease the wear by dissolution of the hard metal in the work piece material. Cracks are easily formed in the hard coatings during production or operation. In order to prevent these cracks from propagating into the substrate it is beneficial to have a relatively high toughness in the surface layer of the substrate. Such a functional gradient in toughness can be accomplished by increasing the volume fraction of binder close to the surface. One way of generating such a microstructure is to dissolve Ti based carbonitrides close to the surface by denitridisation. This will result in a driving force for Ti diffusion towards the centre and diffusion of binder phase formers, *e.g.* Co, to the surface region. In addition to the diffusion generated flow of binder phase there will also be a viscous flow of the binder face driven by differences in surface tension.

The diffusion controlled flow of the binder phase to the surface zone can be simulated utilising the DICTRA software [90And] which is able to predict diffusion in multi component systems by combining mobility data and driving forces computed from thermodynamic models. Utilising the kinetic data and thermodynamic models available to day it is possible to make qualitative predictions of the sintering and functional gradient evolution. The simulation tools have drastically increased the understanding of the controlling mechanisms and have decreased the number of experimental trails in order to optimise materials and production processes. In the future when more reliable thermodynamic data, based on new accurate experiments, are available the simulation methods will be able to provide quantitative predictions.

Thermodynamic modelling combined with kinetic models is today used in several other process steps in the hard metals production, *e.g.* reduction of oxides, syntheses of carbides and reactions between hard metal and tray materials or furnace atmosphere during sintering.

### 3.9 Geo-environmental applications

Processes in geo-environments involve interactions in mineral-fluid (*e.g.*, mineral with aqueous, hydrothermal, geothermal, metamorphic, or magmatic fluid), mineral-mineral (*e.g.*, metamorphic), or mineral-fluid-melt (*e.g.*, magmatic) systems under a variety of pressures, temperatures, and chemical conditions. Thermodynamics provides a powerful tool to simulate these interactions and thereby to quantitatively characterise the operative physical and chemical variables in these processes. The use of thermodynamics in the simulation may be: to predict the final equilibrium state of a multicomponent and multiphase chemical system under specified conditions, to calculate the reaction path wherein the progress of a sequence of reactions is monitored, or to obtain the driving forces or affinities required for a kinetic simulation [93Fle]. In the following sections, we mainly discuss applications of the first category, which is called "speciation" calculation in aqueous geochemistry. We also outline some applications from the other two categories in geochemical modelling. The selection of applications discussed here is not meant to be exhaustive, but intended to provide some pointers only. It should be reiterated, however, that thermodynamics alone can not give a complete description of the process in every case. This is especially true when the reactions are not rapid enough to approximate equilibrium conditions. In such cases, a thermodynamic model should be linked to kinetic and/or other relevant physical models such as heat-flow or fluid dynamics. We may further add that processes resulting from anthropogenic interference with the natural environment are nothing but an extension of the natural processes and can be analysed with the same methodologies that we apply to understand natural phenomena.

#### *Mineral-fluid interactions*

Modelling of reactions between minerals and aqueous, hydrothermal, or other crustal/mantle fluids is important to understand several geochemical processes occurring in the lithosphere and hydrosphere. These processes occur under physical-chemical conditions ranging from those of surface and near-surface (including weathering, diagenesis, geothermal activity, and hydrothermal ore formation) to those at lower crustal and upper mantle levels (effecting metamorphic/metasomatic reactions and igneous activity). Additionally, environmental and social issues such as pollution, contamination by, and containment (geologic disposal) of high-level radioactive and toxic wastes, water and waste water management, and chemical, metallurgical, and mining engineering call for the ability to model mineral-fluid reactions. The modelling usually deals with one or more of the following: dissolution or precipitation of metals, minerals, or other substances; oxidation-reduction reactions; acid-base reactions; and adsorption/desorption of species in the solution with surface functional groups of mineral or organic matter.

There has been an explosion of thermodynamic software designed to calculate mainly heterogeneous equilibria and inorganic speciation in aqueous systems [79Nor, 84Nor]. The popular codes include PHREEQE [80Par], EQ3/EQ6 [83Wol], MINEQL [76Wes], SOLGASWATER [79Eri], WATEQF [76Plu], and GEOCHEM [79Spo]. Thermodynamic software packages ChemSage [90Eri] and Thermo-Calc [85Sun], popular among metallurgists, also have recently included aqueous and fluid species data sets and calculation modules for use in geochemical modelling [93Shi, Thermo-Calc Version L, Newsletter 1996]. The above mentioned programs are members of a family of related codes which represent various improvements and adaptations of an original simpler code. Reference to application of some of the above mentioned thermodynamic codes to the study of natural waters, brines, and soil solutions can be found in [86Nor], [87Wea], and [93Fle].

One of the requirements in applying these codes to geochemical modelling is the availability of quality thermodynamic data for many species. Some of the codes come with their own integrated thermodynamic data sets and model parameters (*e.g.*, EQ3/6, MINEQL, PHREEQE). Many of the available aqueous databases, however, cover a limited number of substances and can be used only for calculating properties at ambient pressure and temperature ($10^5$ Pa and 298.15 K) conditions, and in dilute solutions. In order to model hydrothermal processes, for example, data for a range of species at higher temperatures and pressures are needed. In geochemical research, this is usually done using empirical extrapolation methods such as the Debye-Hückel law, Pitzer model [87Pit], or a method due to Helgeson and co-workers [95Oel]. Independent programs for calculating thermodynamic properties of fluids and aqueous species to higher temperatures and high pressures are available for geological systems (*e.g.*, SUPCRT92 [92Joh], SUPERFLUID [92Bel]).

Although most effort has been aimed at computing inorganic speciation in aqueous systems, there have been also attempts to adapt these codes for handling inorganic-organic complexations [91Fal, 92Har, 96Cra]. Modelling of metal-organic complexation is important in the study of diagenetic and (possibly) low-temperature hydrothermal processes, bio-leaching in mineral processing, and also in evaluating the migration of radioactive nuclides in organic-rich sediments in the context of movement and underground storage of radioactive waste in natural analogue conditions.

Thermodynamic modelling is applied to understand and recommend remedial measures for environmental and industrial problems of the type: scaling and clogging (resulting from mineral precipitation) in ground water treatment plants and oil and gas industry, incorporation of heavy metals and other inorganic toxic components into ground water and secondary minerals, leaching of radionuclides from spent fuel and glass waste forms, evaluation of acid mine waters, corrosion, waste treatment, assessment of contaminated sites, and chemical leaching of ores.

Characterisation of the formation conditions of hydrothermal ore deposits is another area where thermodynamic modelling has found wide applications. Crustal and mantle fluids are responsible for the extraction of metals from the rocks and their subsequent transport and precipitation to form a variety of hydrothermal ore deposits. The ore-forming fluids in their interaction with rocks act as agents of heat and mass transfer. Barring the active hydrothermal systems, these fluids are normally not available for study (except as tiny fluid inclusions in minerals, which may or may not be representative of the ore-forming fluid) in the ore deposits. Thermodynamics, in conjunction with field, mineralogical, and fluid inclusion data, can be used to estimate the ore-forming conditions (*e.g.*, temperature, pH, oxygen and sulphur fugacities, ionic strength). For a detailed review of ore fluids and applications of thermodynamic modelling to the study of ore-forming processes, see [87Bri].

***Metamorphic phase equilibria***

Quantitative characterisation of mineral-mineral and mineral-fluid equilibria using petrologic phase relations and chemical thermodynamics is essential to understanding metamorphic processes. Such characterisation aims at determining the conditions of temperature (geothermometry), pressure (geobarometry), and composition of the fluid phase attending the metamorphism from a knowledge of mineral assemblages and composition of mineral solid solutions coexisting in them. Carefully calibrated thermodynamic activity-composition relations of mineral solid solutions which are sensitive to temperature or pressure are used to work out the temperature or pressure using thermodynamic relations. The estimates of equilibration temperatures and pressures, when correlated with chronological indicators across a metamorphic terrain, reveal the pressure-temperature-time (P-T-t) history of that terrain and provide insights in to its tectonic evolution. See [93Spe] for a list of geothermometers and geobarometers and also several case studies of P-T-t paths. The internally consistent thermodynamic datasets reported in [88Ber], [90Hol2], and [97Got] (and their updates) can be used to calculate thermodynamic properties of end-members of solid solutions, while the activity-composition models of the solutions (which are more scattered in the literature) are incorporated in the geothermometry/geobarometry programs. Software packages specially designed for applications in metamorphic petrology (mainly for geothermometry and geobarometry) include INVEQ [92Gor], THERMOCALC [94Pow], GIBBS [93Spe], and TWEEQU [91Ber].

***Mineral-melt equilibria in igneous petrogenesis***

The major application of thermodynamic modelling in igneous petrology is to quantitatively describe mineral-melt equilibria involved in the melting and chemical differentiation processes such as crystal fractionation, assimilation, and magma mixing that result in the great diversity of igneous rocks. Whereas the thermodynamic properties of most of the rock-forming minerals are well-known, enabling calculations to high temperatures and high pressures (corresponding to lower crustal/upper mantle levels) and as a function of composition, the data and models available to describe the thermodynamics of multicomponent silicate liquids are still inadequate. The main problem with melt modelling is the lack of our understanding of melt structure and speciation under different conditions. Although crystal structural data can be used in the modelling of solid solutions (*e.g.*, the compound energy model), it is not straightforward to use the available structural information on unary, binary, and higher order oxide/silicate liquids [90Mys, 95Mys] in thermodynamic models of liquids. This is principally because of the variable structural roles of components such as $Al_2O_3$, $TiO_2$, and $P_2O_5$ across the composition ranges of magmatic liquids [90Mys] which cause difficulties in systematising the data. The available models use oxide (simple or multiple), mineral-like, or other fictive species as a means to describe the mixing in the liquid solutions. These models are either calibrated for simple binary, ternary, or quaternary synthetic systems (*e.g.*, [84Ber]) or for multicomponent natural magmatic liquid compositions (*e.g.*, [85Ghi]). These two approaches represent a trade off between utility and accuracy: a melt model based on a simple synthetic system is more accurate in itself and may be applicable to a specific rock-type, but not applicable for the wide range of magma compositions that we encounter. A model calibrated on natural lava compositions, on the other hand, can represent a much wider composition range, but may not be accurate enough to extrapolate to simple binaries or ternaries and outside the conditions of calibration.

Even more important than the need for improvements in the thermodynamic models of liquid solutions is the need for accurate thermochemical (heat capacity, enthalpy of fusion, enthalpy of mixing, and component activities) and volumetric (molar volume, thermal expansion, and compressibility) data on a wider range of liquids than that is available [87Ric, 90Lan]. Additionally, more data on the activity-composition relations in mineral solutions are required. These data are required not only to calculate melting temperatures, crystallisation paths, heat budget, geothermometry, geobarometry, and so on, but also to calibrate, extend, and apply melt models to magmatic conditions.

MELTS [95Ghi] is the most comprehensive program available for modelling magmatic processes in the system $SiO_2$-$TiO_2$-$Al_2O_3$-$Fe_2O_3$-$Cr_2O_3$-CaO-MgO-FeO-$K_2O$-$Na_2O$-$H_2O$-$P_2O_5$ under pressures to 4 GPa and temperatures ranging roughly from 1100 to 2000 K. The thermodynamic properties of end-member minerals largely from [88Ber] and recent consistent solid solutions models for igneous rock-forming minerals are included in the software. The mixing in the melt phase is treated by regular solution parameters. The authors indicate that with MELTS, calculations of equilibrium or fractional crystallisation; crystallisation paths under constrained temperature - oxygen fugacity, total enthalpy, total entropy, total volume, (or any combination of these) conditions; isothermal, isenthalpic, or isochoric assimilation, magma mixing, and degassing of volatiles can be performed. An additional feature of MELTS is the facility to revise the melt model parameters when additional data become available. Examples of the use of MELTS in thermodynamic modelling of igneous systems may be found in [97Ghi].

MELTS and other similar programs have been calibrated for mixing among major constituents in the melt. It is also possible to derive petrogenetic constraints by modelling the trace element partitioning between melts and crystals. Nielsen [90Nie] has discussed the use of phase equilibria constraints in modelling the igneous processes using major and trace element data. It appears that formulation of multicomponent melt models with structural information is a difficult task at the moment. Future work must include formulation of multicomponent liquid models that could handle both major and trace element behaviour in magmas, major dissolved fluid species, ordering tendencies, and liquid immiscibility.

***Mantle mineralogy***

A knowledge of the physical and chemical nature of the Earth's interior is essential for our understanding of its dynamic behaviour that leads to various phenomena such as plate tectonics, volcanism, and earth quakes. Although the general structure of the Earth's interior has been known for some time through the study of seismic

wave velocities, the real chemical and mineralogical constitutions at various depths inside the Earth is not known. Thermodynamic analyses of possible mineralogical variations with depth on inferred mantle and core chemical compositions have been lacking until recently mainly because of the paucity of sufficient thermochemical, thermophysical, and phase equilibrium data on relevant systems. Phase equilibria in the model system CaO-MgO-FeO-$Al_2O_3$-$SiO_2$ to 30 GPa and 3000 K and the pressure-volume-temperature (P-V-T) relations of many of the candidate mantle minerals have been measured in the recent past and are reviewed by [92Ita], [93Sax], and [96Sax]. Thermochemical data for high-pressure phases are a major lacuna, even though some attempts have been made to create consistent data sets using the published phase equilibria and P-V-T data along with other available physical data [92Ita, 93Sax]. For example, even for an important phase like $CaSiO_3$-perovskite, believed to be the sole host of Ca under a range of mantle pressure-temperature conditions, there is only a preliminary thermodynamic data set obtained recently by [97Swa] by combining CALPHAD assessment with semi-empirical atomistic simulation to estimate thermophysical properties. The principal reasons for the lack of measured data on high-pressure phases such as $CaSiO_3$-perovskite include the difficulties associated with metastability (amorphisation) at ambient conditions and synthesis in large amounts for use in calorimetric measurements. Prediction of the properties using atomistic simulation methods appears to be promising (*e.g.*, [95Wen, 96Bel]).

With the available phase equilibria, calorimetry, and thermophysical data and relying on extrapolations to mantle pressures and temperatures using sound physical theories, there have been some recent attempts to model equilibrium mantle mineralogy. For the transition zone between Earth's upper and lower mantle, two chemical models namely, pyrolite and piclogite, two chemical models were analysed by [92Ita] by combining the available phase equilibria and mineral elasticity data in the CaO-MgO-FeO-$Al_2O_3$-$SiO_2$ system in a self-consistent semiempirical thermodynamic formalism. Mie-Grüneisen and Birch-Murnaghan equations of state were combined with ideal solution theory to extrapolate experimental measurements to pressures and temperatures of the mantle. With these data, the density, seismic parameter, and mantle adiabats were calculated for both chemical compositions. The pyrolite and piclogite compositions can both account for the steeper velocity and density gradients in the transition zone, with pyrolite having a better agreement with the seismic observations throughout the upper mantle and transition zone. [92Ita] suggested that the conversion of garnet to $CaSiO_3$-perovskite near 18 GPa may explain the proposed seismic discontinuity at a depth of 520 km. They further observed that below 700 km depth, all investigated compositions disagree with observed velocities, implying that the lower mantle is chemically distinct from the upper mantle.

Another similar effort is that of [96Sax] who computed the mineral assemblages in the MgO-FeO-$SiO_2$ system (in peridotitic/pyrolitic and chondritic proportions) along a mantle adiabat by employing the ChemSage Gibbs energy minimiser [90Eri]. For this purpose, an internally consistent thermochemical and equation of state data base was first created using the CALPHAD analysis of available phase equilibrium, calorimetric, and physical measurements. The pressure contribution to the Gibbs energy of each individual phase was modelled using a high-temperature Birch-Murnaghan equation of state. The computed density variations along the adiabatic gradient showed remarkable similarity to the densities given by the standard Preliminary Reference Earth Model (PREM), which was obtained by the inversion of a large set of seismic data [81Dzi]. The computed densities showed similar discontinuities corresponding to mineral reactions or phase transitions, however, not as sharp as the seismic discontinuities. The general similarity of the seismic and mineralogical density profiles corroborate the inference that phase transitions are dominantly responsible for the presence of the seismic discontinuities in the mantle. This is an important result because two totally independent models namely, mineralogical and seismic, are revealing an identical picture of the density of the Earth's interior [96Sax].

***Coupling of thermodynamic and other models***

As mentioned earlier, a more complete understanding of some processes is achieved only when a thermodynamic model is coupled with a kinetic or other physical model. Some geological examples of such cases are: weathering, role of heat flow in metamorphism, and fluid dynamics in a magma chamber. The coupling may be done through a general interface that transfers data between the thermodynamic code and the "non-thermodynamic" software, as is the case with the ChemApp (TQ) interface mentioned elsewhere. Alternatively, a custom-made program may be built around an existing thermodynamic code. Although the first approach is preferable because it requires minimum or no modification to the thermodynamic and the "non-thermodynamic" software (especially if they are commercial), several of the adaptations of the aqueous geochemistry codes mentioned earlier represent the latter one. We discuss below some examples from geochemical modelling of fluid-rock interactions.

In complex aqueous solutions, the speciation of dissolved material (solutes) vary as a function of environmental factors such as pH, ionic strength, chemistry of the solution, pressure, temperature, and redox condition. Speciation codes can be used to characterise the nature and abundance of various species under varying conditions. These data can then be used in further modelling, normally using a coupled code. For example, MINEQL and PHREEQE codes have been adapted to calculate adsorption equilibrium between the dissolved chemical species, obtained in the speciation calculation, and surface functional groups of the undissolved minerals or natural organic matter [76Wes, 90Bro].

In reaction path or reaction progress calculations, the speciation calculation is performed in successive stages to characterise the subsidiary reactions that lead to the final equilibrium. EQ3/6 is widely used to perform reaction path calculations. It combines speciation calculation (EQ3) with mass transfer and reaction progress (EQ6). Other examples from aqueous geochemistry include the programs CHEQMATE [85Mul] and CRACKER [91Emr] which couple chemistry with transport (one-dimensional diffusion and ion migration) and use PHREEQE to do the speciation calculation.

An example of integrated modelling of ore-forming process is the work of Cunningham (1984) (cited in [87Bri]) to model irreversible reaction path of supergene copper enrichment in a pyrite-chalcopyrite-magnetite-biotite-alkali feldspar protore by combining the EQ3/6 with a fluid flow model. This modelling effort integrated thermodynamic, kinetic (Fick's first law type equation was used in this study to describe oxygen diffusion in the capillary fringe), and fluid flux data to compute reaction chemistry in a supergene enrichment process. The results of the calculation were consistent with petrographic data from the ore zone, suggesting that geologically meaningful analysis can be performed with such approaches.

The next two examples deal with modelling of hydrothermal alteration processes. Reaction-path modelling was performed by [98McC] with EQ3/6 to investigate the alteration in the mineral assemblages produced by fluid-rock interactions during circulation of seawater into hot lower oceanic crust. Thermodynamic data for the gases, minerals, aqueous species, and complexes in the system Na-Ca-Mg-Fe-Al-Si-O-H-Cl chosen for this study were from SUPCRT92 [92Joh]. The predicted alteration assemblages for reactions involving an evolving seawater with olivine gabbro, gabbronorite, and troctolite during heating from 300 to 900 °C closely resembled the alteration assemblages observed in the lower oceanic crustal rocks.

A combined thermodynamic and hydrodynamic model was used by [97Tut] to simulate modern hydrothermal systems ("black smokers") in mid-ocean ridges. The hydrodynamic part of the model used numerical solution of Darcy's law and heat transfer equation by the finite element method. A flow-type stepwise reactor model was used in the thermodynamic part. Local equilibrium between solution and wall rocks in the system Na-K-Ca-Mg-Fe-Al-Si-C-S-Cu-Zn-Pb-O-H-Cl were calculated at each step. The spatial distribution of the secondary mineral assemblages obtained in the study is generally similar to those observed in the oceanic hydrothermal systems.

***Environmental application: An illustrative example***

Toxic dioxins and furans are unintentionally formed in a number of industrial combustion processes such as waste incineration and iron ore sintering, in the chemical industry, and in household heating. As an example, during operation of an industrial sinter plant, analyses of the waste gases passing the filter system show negligible dioxin content. However, the dioxin levels measured in the wind boxes situated beneath the sinter strand itself are significant.

A straightforward equilibrium calculation with big organic molecules would always give us a result that the equilibrium amounts of these are way below the experimentally obtained values. However, making certain assumptions with regard to the reactive oxygen, carbon, and water vapour at different positions along the sinter strand, it was possible to calculate off-gas compositions and dioxin concentrations in close agreement with measured values [97Eri].

The calculations were made using ChemApp (the TQ interface linked with ChemSage) and based on the sinter strand arrangements shown in Figure 3.9.1. The ore mixture containing coke is fed onto the travelling grate and then ignited using a gas mixture consisting of air, blast furnace gas, and natural gas. As the sinter strand moves along, air is drawn through the bed, causing the ignition front to move downwards through the bed. The speed of

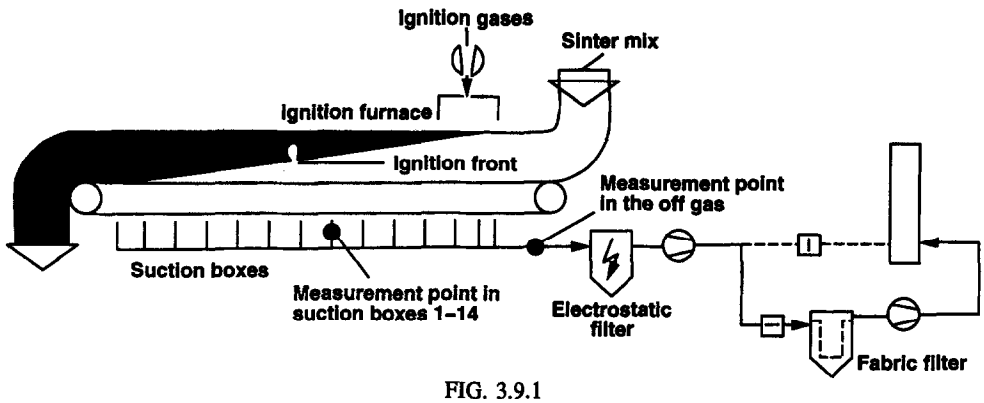


FIG. 3.9.1
Off gas system of the sinter plant

the grate is adjusted such that the sinter process is complete when the mixture reaches the end of the strand. Beneath the grate and along its length are 14 suction boxes in which the gases passing through the sinter bed as well as the materials condensing from them are collected for analysis of CO, $CO_2$, $O_2$, $H_2O$, and dioxins.

The successful simulation of the off-gas composition indicates that at 700 °C the gas phase reactions can be considered as 'frozen in' Pand it was therefore decided that simulation of dioxin formation should also be carried out for this temperature.

Dioxins are metastable compounds that only exist whenever the formation of solid carbon is suppressed. The calculations further indicate that dioxins only start to form in the amounts observed in practice if two further assumptions are made:

(1) the oxygen partial pressures must be set to very low values, or, equivalently, the carbon activities to very high values
(2) the C/H ratio must be greater than 2, which implies that a large part of the hydrogen present does not take part in the reaction.

## 4. Current software interfaces

The increasing level of sophistication in process modelling makes it highly desirable to use more realistic phase equilibria information instead of simplified approximations. This kind of phase equilibria information can be obtained from computational thermodynamics codes which can be coupled to the process modelling computer codes. For this software coupling an interface must be created in which the important variables are transferred from one code segment to another. An example for such an interface is the TQ (ChemApp) interface [94Eri] discussed below.

The use of repetitive thermochemical calculations for solving practical problems in many different technological fields has grown considerably in recent years. Detailed models have been developed, both for the processes mentioned in Table I and for the thermochemical properties of solution phases as a function of pressure, temperature, and composition. The software packages used thus tend to increase in number and size and there is a need to separate them into well defined interfaces.

The more sophisticated modelling of solutions and alloys also makes it imperative to use a separate thermodynamics software. A consistent and reliable description of the equilibrium and the thermodynamic quantities can then be obtained.

Several of the commercially available process simulation packages, for example, Phoenics and Fluent for computational fluid dynamics (CFD), and Aspen and Process for flow-sheeting, just to mention a very few, would benefit from incorporating an efficient and well established code for Gibbs-energy minimization to predict the

stable assembly of phases at chemical equilibrium for given input conditions. The Gibbs-energy minimizers most widely used include ChemSage [90Eri], MTDATA [91Dav], and Thermo-Calc [85Sun].

Under the auspices of an EC-Science project involving RWTH Aachen (ChemSage), KTH Stockholm (Thermo-Calc), and HUT Helsinki, a generalized thermodynamic subroutine library, namely TQ interface, was developed [94Eri]. Linked either to the phase equilibrium modules of ChemSage or Thermo-Calc, the interface can be added as a chemical equilibrium computation module to any third-party process simulation package. The purpose of the interface is thus to serve as a communication link between the process simulation package and the Gibbs energy minimizer.

There are some desirable features to any software interface: First, it has to be easily understood and used by the application programmer. Secondly, it has to be available in a form such that the programmer can use a language and a platform he or she finds convenient. In the course of a process simulation, the TQ interface might be called to make a Gibbs-energy minimization thousands of times, for instance to calculate local equilibrium or boundary conditions. It thus has to be fast and reliable and must seldom fail to converge.

Essentially, only four programming steps are necessary to proceed from initialization of the interface to collection of results.

(1) Initialisation of the interface and reading a data-file containing thermochemical data for the actual system. The format of this file depends on the Gibbs-energy minimizer to the interface.
(2) Asking for details on the chemical system, *e.g.*, total number of phases or the index number of a phase constituent. During this step phases can also be defined as metastable.
(3) Setting the conditions for the calculation. In the simplest case this just means defining temperature, pressure, and input amounts. If input streams with given temperatures and pressures are defined, enthalpy balances can be calculated. Adiabatic temperatures can be calculated if a zero enthalpy balance is given as input. Eutectic temperatures are calculated if, instead of temperature, the driving force of the liquid phase at equilibrium is specified as being zero.
(4) Performing the complex equilibrium calculation and collecting results.

The TQ interface, consisting of about 35 subroutines, represents the lowest level of access to the Gibbs-energy minimizer, allowing modification of individual conditions and the selection of a set of components and phases. In many cases a more straightforward technique can be used. For example, Banerjee *et al.* (97Ban) have implemented a thermodynamic software interface with just 4 subroutines. In this case only temperature and composition can be used as input conditions and obtained as results. This interface can be easily incorporated on top of the TQ interface, thus making it possible to handle problems of a certain type without understanding the details of the TQ interface.

Another interface is the Application Interface of MTDATA [98Din]. This interface provides a series of functions and subroutines which are intended to be both self documenting and comprehensive. The names of the routines in this interface are generally verbose in order to allow source code which is easy to understand and manage.

## 5. Conclusion

Although a wide variety of application examples has been presented in the present overview, it is by no means exhaustive. Generally two different groups of applications can be distinguished, direct and indirect applications. In the direct applications computational thermodynamics is used to generate phase diagrams of diagrams with thermodynamic functions that can be used to modify or adjust process parameters. This area is relatively mature and will continue to be an important tool since it provides simultaneously the basis for data development and indirect applications. In the indirect applications computational thermodynamics is linked with other modelling or simulations software, providing some of the data that are needed. Indirect applications, such as in process modelling, are emerging and gaining increased importance. With indirect application the utilization of computational thermodynamics may not be obvious to the user since it is used within the computer code to provide data needed for the process modelling or simulation. However, this requires that software and database be very robust in order to produce reliable data. Presently, direct applications are the majority, however, the

number of indirect application increases steadily, partly because of the growing capabilities of computers, which are needed for reasonable response times.

**References**


[33Dix] E.H. Dix, W.L. Fink, and L.A. Willey, Trans. AIME 104 (1933) 335.

[43Phi] H.W.L. Phillips, J. Inst. Metals 69 (1943) 275.

[59Phi] H.W.L. Phillips, "Annotated Equilibrium Diagrams of Some Aluminium Alloys Systems," Monograph and Report Series, No 25, The Institute of Metals, London, (1959).

[61Phi] H.W.L. Phillips, "Equilibrium Diagrams of Aluminium Alloys Systems," The Aluminium Development Association, London, (1961).

[71God] T. Gödecke and W. Köster, Z. Metallkde. 62 (1971) 727.

[72Pan] M.B. Panish and M. Ilegems, Prog. Solid State Chem. 7 (1972) 39.

[74Sig] G.K. Sigworth and J.F. Elliott, Metal Science 8 (1974) 298.

[76Mon] L.F. Mondolfo, "Al Alloys; Structure and Properties", Butterworths, London & Boston, (1976).

[76Plu] L.N. Plummer, B.F. Jones, and A.H. Truesdell, "WATEQF- a FORTRAN IV version of WATEQ, a computer program for calculating chemical equilibrium of natural waters," U.S. Geol. Surv. Water-Resources Investigations Report 76-13, (1976).

[76Wes] J. Westall, J.L. Zachary, and F.M.M. Morel, "MINEQL, a computer program for the calculation of chemical equilibrium composition of aqueous systems," Mass. Inst. Tech. Dept. Civil Eng. Tech. Note 18, 1996.

[79Eri] G. Eriksson, Anal. Chim. Acta 25 (1979) 2651.

[79Nor] D.K. Nordstrom, L.N. Plummer, T.M.L. Wigley, T.J. Wolery, J. W. Ball, E.A. Jenne, R.L. Bassett, D.A. Crerar, T.M. Florence, B. Frtiz, M. Hoffman, G.R. Holdren, Jr., G.M. Lafon, S.V. Mattigod, R.E. McDuff, F. Morel, M.M. Reddy, G. Sposito, and J. Thrailkill, "A comparison of computerized chemical models for equilibrium calculations in aqueous systems," in: *Chemical Modelling in Aqueous Systems*, E.A. Jenne (ed.), p. 857, American Chemical Society Symposium (Series 93), (1979).

[79Spo] G. Sposito and S.V. Mattigod "GEOCHEM: A computer program for the calculation of chemical equilibria in soil solution and other natural water systems," Dept. Soil Environ. Sci., University of California, (1979).

[80Par] D.L. Parkhurst, D.C. Thorstenson, and L.N. Plummer "PHREEQE - a computer program for geochemical calculations," U.S. Geol. Surv. Water-Resources Investigations Report 80-96, (1980, revised and reprinted, 1990).

[81Dzi] A.M. Dziewonski and D.L. Anderson, Phys. Earth Planet. Inter. 25 (1981) 297.

[83And] T.J. Anderson, "Chemical Vapor Deposition of Semiconductor Materials," AIChE Symp. Series 229, 79, p. 150 (1983).

[83Wol] T.J. Wolery, "EQ3NR: a computer program for geochemical aqueous speciation-stability calculations: theoretical manual, user's guide, and related documentation (Version 7)," Lawrence Livermore National Laboratory Report UCRL-MA-110662-PT-III, (1983).

[84Ber] R.G. Berman and T.H. Brown, Geochim. Cosmochim. Acta 45 (1984) 661.

[84Gay] H. Gaye and J. Welfringer, "Modelling of the thermodynamic properties of complex metallurgical slags," Second International Symposium on Metallurgical Slags and Fluxes, Lake Tahoe, Nevada, TMS-AIME, (1984).

[84Nor] D.K. Nordstrom and J.W. Ball, "Chemical models, computer programs and metal complexation in natural waters," in: *International symposium on trace metal complexation in natural waters*, C.J.M. Kramer and J.C. Duinker (eds.), p. 149, Martinus Nijhoff/Dr. J.W. Junk Publishing Co., (1984).

[85Ase] T.L. Aselage, K.M. Chang , and T.J. Anderson, "Solid-Liquid Equilibrium in Multicomponent Group III-V Semiconductor Materials," ACS Symposium Series, 290, p. 276, (1985).

[85Ghi] M.S. Ghiorso, Contrib. Mineral. Petrol. 90 (1990) 107.

[85Hes] D.W. Hess, K.F. Jensen, and T.J. Anderson, Reviews Chem. Eng. 3 (1985) 97.

[85Mul] A.B. Muller, D.L. Parkhurst, and P.W. Tasker, "The use of the PHREEQE code in modelling environmental geochemical problems encountered in performance assessment modelling," in: *Proceedings of Symposium on Groundwater Flow and Transport Modelling for Performance Assessment of Deep Geologic Disposal of Radioactive Waste: A Critical Evaluation of the State of the Art.* Albuquergue, New Mexico, (1985).

[85Sun] B. Sundman, B. Jansson, and J.-O. Andersson, Calphad 9 (1985) 153.

[86Bak] L. Bäckerud, E. Krol, J. Tamminen, "Solidification Characteristics of Aluminium Alloys, Vol. 1: Wrought Alloys," Skanaluminium, (1986).

[86Hil] M. Hillert, Metall. Trans. A 17A (1986) 1878.

[86Nor] D.K. Nordstrom and J. Munoz, "Geochemical Thermodynamics," Blackwell Scientific, Palo Alto, (1986).

[86Pel] F. Pellicani, F. Villette, and J. Dubois, "The production of clean, isotropic steel by means of calcium treatment with the Affival cored-wired," in: *Proceedings of ScanInject 4*, MEFOS, Lulea Sweden, (1986).

[86Sau] N. Saunders and A.P. Miodownik, J. Mater. Res. 1 (1986) 38.

[86Smi] N.K. Smit, G.A. Acket, and C.J. van der Laan, Thin Solid Films 138 (1986) 171.

[86Ues] Y. Ueshima, S. Mizoguchi, T. Matsumiya, and H. Kajioka, Metall. Trans. B 17B (1986) 845.

[87Bri] G.H. Brimhall and D.A. Crerar "Ore fluids: Magmatic to supergene," in: *Thermodynamic Modeling of Geological Materials: Minerals, Fluids, and Melts*, Rev. Mineral. 17, I.S.E. Carmichael and H.P. Eugster (eds.), p. 235, Mineralogical Society of America, (1987).

[87Cha] S. Chang, D. Unzicker, and T.J. Anderson, "A Thermodynamic Analysis of CVD of Ge-Si in the Ge-Si-Cl-H System," in: *Proc. Tenth Int. Conf. on CVD*, p. 122 (1987).

[87Flo] S.C. Flood and J.D. Hunt, J. Crystal Growth 82 (1987) 543.

[87Deo] B. Deo, P. Ranjan, and A. Kumar, Steel Research 58(9) (1987) 427.

[87Gay] H. Gaye, C. Gatellier, M. Nadif, P.V. Riboud, J. Saleil and M. Faral, Revue Metallurgie CIT (11) (1987) 759.

[87Kno] O. Knotek and T. Leyendecker, J. Solid State Chem. 70 (1987) 318.

[87McA] A.J. McAlister, J.L. Murray, Bull. Alloy Phase Diag. 8 (1987) 438.

[87Mur] J.L. Murray (ed), "Phase Diagrams of Binary Titanium Alloys," ASM International, (1987).

[87Pit] K.S. Pitzer "A thermodynamic model for aqueous solutions of liquid-like density," in: *Thermodynamic Modeling of Geological Materials: Minerals, Fluids, and Melts*, Rev. Mineral. 17, I.S.E. Carmichael and H.P. Eugster (eds.), p. 97, Mineralogical Society of America, (1987).

[87Rap] M. Rappaz and Ph. Thévoz, Acta Metall. 35 (1987) 1487.

[87Ric] P. Richet and Y. Bottinga, Rev. Geophysics 24 (1986) 1.

[87Wan] D.H. Wang, in: *Proc. 172nd Meeting of the Electrochemical Society*, Hawaii, Oct.1987, Electrochem. Soc., 2, p. 575, (1987).

[87Wea] J.H. Weare "Models of mineral solubility in concentrated brines with application to field observations," in: *Thermodynamic Modeling of Geological Materials: Minerals, Fluids, and Melts*, I.S.E. Carmichael and H.P. Eugster (eds.), Rev. Mineral. 17, p. 143, Mineralogical Society of America, (1987).

[88And] T.J. Anderson, "Examples of Chemical Engineering Principles Applied to the Growth of Semiconductors," in: *Chem. Eng. Ed. in a Changing Environment*, S.I. Sandler and B.A. Finlayson (eds.), p. 311, AIChE Publ., (1988).

[88Ber] R.G. Berman, J. Petrol. 29 (1988) 445.

[88Cos] A. Costa e Silva and P.R. Mei, "Steels and Specialty Alloys" (in Portuguese), Eletrometal, Sumare, Brasil, (1988).

[88Nay] A.A. Nayeb-Hashemi, J.B. Clark (eds.), "Phase Diagrams of Binary Magnesium Alloys," ASM International, (1988).

[88Rap] M. Rappaz and D.M. Stephanescu, in: *CASTING, ASM Handbook, Vol. 15*, p. 883, ASM, Metals Park, OH, (1988).

[88Sch] H. Schüle and W.-I. Ratzel, "Technische Keramik", 1st Edn., Vulkan, Essen, (1998).

[88Wan] D.H. Wang and L. Guo, Thin Solid Films 158 (1987) L39.

[89And] T.J. Anderson, "Liquid Phase Epitaxy and Phase Diagrams of Compound Semiconductors," in: *Advances in Chemistry Series No. 221: Chemical Engineering in Electronic Materials Processing*, p. 105, (1989).

[89Rap] M. Rappaz, Int. Mat. Rev. 34 (1989) 93.

[89Sha] Y.G. Sha and R.F. Brebrick, J. Electron. Mater. 18 (1989) 421.

[89Ues] Y. Ueshima, H. Yuyama, S. Mizoguchi, and H. Kajioka, Tetsu-to-Hagane 75(3) (1989) 501.

[89Zol] M.E. Zolensky, W.L. Bourcier, and J.L. Gooding, Icarus 78 (1989) 411.

[90And] J.-O. Andersson, L. Höglund and B. Jönsson, in: *Fundamentals and Applications of Ternary Diffusion*, G.R. Purdy (ed.), p.153, Pergamon, New York, (1990).

[90Bak] L. Bäckerud, G. Chai, J. Tamminen, "Solidification Characteristics of Aluminium Alloys, Vol. 2: Foundry Alloys," Skanaluminium, (1990).

[90Bro] P. L. Brown, A. Haworth, S. M. Sharland, and C. J. Tweed, "HARPHRQ: An extended version of the geochemical code PHREEQE," NIREX Safe Studies Rept. NSS-R. 188, Harwell Laboratory, Oxfordshire, U. K., (1990).

[90Eri] G. Eriksson and K. Hack, Metall. Trans. B 21B (1990) 1013.

[90Gio] B. Giovanola and W. Kurz, Metall. Trans. A 21A (1990), 260.

[90Holl] P.H. Holloway and T.J. Anderson (eds.), "Compound Semiconductors: Growth, Processing and Devices," CRC Press, Boca Raton, FL (1990).

[90Hol2] T.J.B. Holland and R. Powell, J. metamor. Geol. 8 (1990) 89.

[90Lan] R. L. Lange, and I. S. E. Carmichael, "Thermodynamic properties of silicate liquids with emphasis on density, thermal expansion and compressibility," in: *Modern Methods of Igneous Petrology: Understanding Magmatic Processes*, J. Nicholls and J. K. Russell (eds.). Rev. Mineral. 24, p. 25, (1990).

[90Loo] F.J.J. van Loo, Prog. Solid St. Chem., 20, (1990) 47.

[90Mas] T.B. Massalski (ed), "Binary Alloy Phase Diagrams," 2nd Edn., ASM International, (1990).

[90Mys] B.O. Mysen, Earth Sci. Rev. 27 (1990) 281.

[90Nie] R.L. Nielsen, "Simulation of igneous differentiation processes," in: *Modern Methods of Igneous Petrology: Understanding Magmatic Processes*, J. Nicholls and J.K. Russell (eds.), Rev. Mineral. 24, p. 65, (1990).

[90Pet] G. Petzow, G. Effenberg (eds.), "Ternary Alloys," VCH Weinheim & New York, Vol. 3, (1990), see also Vol. 4, (1991), Vol. 5, (1992), Vol. 6, (1993), Vol. 7, (1993), Vol. 8, (1993).

[90Spe] P.J. Spencer and H. Holleck, High Temp. Science 27 (1990) 295.

[91Ber] R.G. Berman, Canad. Mineral. 29 (1991) 833.

[91Cao] W.D. Cao, R.L. Kennedy, and M.P. Willis, in: *Superalloys 718, 625 and Various Derivatives*, E.A. Loria (ed.), p. 147, TMS, Warrendale, PA, (1991).

[91Dav] R.H. Davies, A.T. Dinsdale, S.M. Hodson, J.A. Gisby, N.J. Pugh, T.I. Barr, and T.G. Chart, "MTDATA - The NPL Databank for Meatllurgical Thermochemistry," in: *User Aspects of Phase Diagrams*, F. H. Hayes (ed.), p. 140, The Institute of Metals, London, (1991).

[91Emr] A. Emrén, Radiochim. Acta 53 (1991) 473.

[91Fal] W.E. Falck, Comp. Geosci. 17 (1991) 1219.

[91Ker] D.M. Kerrick, in: *Contact Metamorphism*, Rev. Mineral. 26, p. 847, Mineralogical Society of America, (1991).

[91Nak] T. Nakakita, K. Shinchi, and T. Tagami, "End point control system at Nippon Steel Corporation", Sublance and Dynamic Control Steelmaking Conference, Hoogovens, Hoogovens IJmuiden (1991).

[91Pet] G. Petzow and K.G. Nickel, "Phase Diagrams: Tools for the Development of Advanced Ceramics," in: *User Aspects of Phase Diagrams*, F. H. Hayes (ed.), p. 40, The Institute of Metals, London, (1991).

[92Agr] J. Ågren, ISIJ International, 32 (1992) 291.

[92And] J.-O. Andersson and J. Ågren, J. Appl. Phys. 72 (1992) 1350.

[92Bat] T.P. Battle, International Mater. Rev. 37(6) (1992) 249.

[92Bel] A.B. Belonoshko, P. Shi, and S.K. Saxena, Comp. Geosci. 18 (1992) 1267.

[92Cor] H. Cordes and R. Schmid-Fetzer, Z. Metallkde. 83 (1992) 601.

[92Gat] C. Gatellier, H. Gaye, J. Lehmann, J. Bellot, and M. Moncel, La Revue de Metallurgie (4) (1992) 362.

[92Gor] T.M. Gordon, Geochim. Cosmochim. Acta 56 (1992) 1793.

[92Har] W.J. Harrison and G.D. Thyne, Geochim. Cosmochim. Acta 56 (1992) 565.

[92Hil] M. Hillert and S. Jonsson, Z.Metallkde 83 (1992) 714.

[92Ita] J. Ita and L. Stixrude, J. Geophys. Res. 97(B5) (1992), 6849.

[92Jan] A. Jansson, Metall. Trans. A 23A (1992) 2953.

[92Joh] J.W. Johnson, E.H. Oelkers, and H.C. Helgeson, Comp. Geosci. 18 (1992) 899.

[92Kno] W. v. D. Knoop, B. Deo, A.B. Snoeijer, G. v. Unen, and R. Boom, "A dynamic slag-droplet model for the steelmaking process," 4th International Conference on Molten Slags and Fluxes, Sendai, Japan, ISIJ, (1992).

[92Li] X.L. Li, R. Hillel, F. Teyssandier, S.K. Choi, and F.J.J. van Loo, Acta Metall. 40, (1992) 3149.

[92Mat] T. Matsumiya, Mater. Trans. JIM 33(9) (1992) 783.

[92Zha] M.-X. Zhang, K.-C. Hsieh, J. DeKock, and Y.A. Chang, Scr. Metall. 27 (1992) 1361.

[93Cho] K. C. Chou, U.B. Pal, and R.G. Reeddy, ISIJ International 33(8) (1993), 862.

[93Deo] B. Deo and R. Boom, "Fundamentals of steelmaking metallurgy," Prentice Hall, (1993).

[93Fle] P. Fletcher, "Chemical Thermodynamics for Earth Scientists," Longman Scientific & Technical, Hong Kong, (1993).

[93Gen] C. Gente, M. Oehring, and R. Bormann, Phys. Rev. B 48 (1993), 13244.

[93Hum] G. Humpston and D.M. Jacobson, "Principles of Soldering and Brazing," ASM International, Materials Park, Ohio (1993).

[93Kub] O. Kubaschewski, C.B. Alcock, and P.J. Spencer, " Materials Thermochemistry," Pergamon Press, Oxford, (1993).

[93Sax] S.K. Saxena, N. Chatterjee, Y. Fei, and G. Shen, "Thermodynamic Data on Oxides and Silicates," Springer-Verlag, Berlin, Heidelberg, New York, (1993).

[93Sel] M. Selleby, "Thermodynamic Modelling and Evaluation of the Ca-Fe-O-Si System," Royal Institute of Technology, KTH, Stockholm, (1993).

[93Shi] P. Shi, "Thermodynamics of the C-H-O-S fluids with some applications," Unpublished Ph. D. Thesis, Uppsala University, Sweden, (1993).

[93Spe] F.S. Spear, "Metamorphic phase equilibria and pressure-temperature-time paths," Mineralogical Society of America, Washington, D.C., p. 799, (1993).

[93Sto] H. Stolten, P.J. Spencer, and D. Neuschütz, J. Chim. Phys. 90 (1993) 209.

[93Via] P.T. Vianco and D.R. Frear, JOM 45 (1993) 14.

[93Wen] H. Wenzl, W.A. Oates, and K. Mika, in: *Handbook of Crystal Growth*, D.T.J. Hurle (ed.), Vol. 1A, p. 103, North-Holland, Amsterdam, (1993).

[94Ans] I. Ansara, C. Chatillon, L. Lukas, T. Nishizawa, H. Ohtani, K. Ishida, M. Hillert, B. Sundman, B.B. Argent, A. Watson, T.G. Chart, and T.J. Anderson, CALPHAD 18 (1994) 117.

[94Bor] R. Bormann, "Kinetics of Interface Reactions in Polycrystalline Thin Films," in: *Polycrystalline Thin Films*, K. Barmak, M.A. Parker, J.A. Floro, R. Sinclair, and D.A. Smith (eds.), Mat. Res. Soc. Symp. Proc. 343, p. 169, (1994).

[94Eri] G. Eriksson, H. Sippola, and B. Sundman, "A Proposal for a General Thermodynamic Software Interface," in: *Proceedings of the Colloquium on Process Simulation*, Helsinki University of Technology, Report TKK-V-B99, p. 67, (1994).

[94Gan] Ch.-A. Gandin and M. Rappaz, Acta Metall. Mater. 42 (1994) 2233.

[94Hal] B. Hallstedt, M. Hillert, M. Selleby, and B. Sundman, CALPHAD 18 (1994) 31.

[94Han] Q. Han and R. Schmid-Fetzer, Mater. Sci. Eng. B22 (1994) 141.

[94Ogi] S. Ogibayashi, "Advances in technology of oxide metallurgy," in: *Nippon Steel Technical Report 61*, p. 70, (1994).

[94Pow] R. Powell and T.J.B. Holland, Amer. Mineral. 79 (1994) 120.

[94Sau] N. Saunders, presented at Symposium on Applications of Thermodynamics in the Synthesis and Processing of Materials, Materials Week 1994, Rosemont, IL.

[95Ans] I. Ansara, "Thermochemical Database for Light Metal Alloys," COST 507, Concerted Action on Materials Sciences, European Commission, DG XII, Luxembourg, (1995).

[95Boe] W.J. Boettinger, U.R. Kattner, S.R. Coriell, Y.A. Chang, and B.A. Mueller, in: *Modelling of Casting, Welding and Advanced Solidification Processes VII*, M. Cross and J. Campbell (eds.), p. 649, TMS, Warrendale, PA, (1995).

[95Bri] J. K. Brimacombe and I. Samarasekera, "The Continuous Casting of Steel," a Short Course presented at UFF, UFF/ABM, Volta Redonda, RJ, Brasil, (1995).

[95Bus] R. Busch, F. Gaertner, C. Borchers, P. Haasen, and R. Bormann, Acta metall. mater. 43 (1995) 3467.

[95For] R.K. Foran, T. Hansen, and B. Mueller, in: *Modelling of Casting, Welding and Advanced Solidification Processes VII*, M. Cross and J. Campbell (eds.), p. 771, TMS, Warrendale, PA, (1995).

[95Ghi] M.S. Ghiorso and R.O. Sack, Contrib. Mineral. Petrol. 119 (1995) 197.

[95Goe] F. Goesmann and R. Schmid-Fetzer, Semicond. Sci. Technol. 10 (1995) 1652 and 11 (1996) 461.

[95Ito] T. Ito, J. Appl. Phys. 77 (1995) 4845.

[95Kou] P. Koukkari, "A Physico-Chemical Reactor Calculation by Successive Stationary States," Acta Polytechn. Scand., Chem. Tech. Series No. 224, (1995).

[95Lin] C.-F. Lin, Y.A. Chang, N. Pan, J.-W. Huang, and T.F. Kuech, Appl. Phys. Letters 67 (1995) 3587.

[95Mat] K. Matsuura, M. Kudoh, and T. Ohmi, ISIJ International 35(6) (1995) 624.

[95Moh] S.E. Mohney and Y.A. Chang, J. Appl. Phys. 78 (1995) 1342.

[95Mys] B.O. Mysen, Eur. J. Mineral. 7 (1995) 745.

[95Oel] E.H. Oelkers, H.C. Helgeson, and V.A. Pokrovskii, J. Phys. Chem. Ref. Data 24 (1995) 1401.

[95Ohs] K. Ohsasa, S. Nakaue, M. Kudoh, and T. Narita, ISIJ International 35(6) (1995) 629.

[95Ste] D. M. Stefanescu, ISIJ International 35(6) (1995) 637.

[95Tho] B. G. Thomas, ISIJ International 35(6) (1995) 737.

[95Tie] T.-Y. Tien, "Use of Phase Diagrams in the Study of Silicon Nitride Ceramics," in: *Phase Diagrams in Advanced Ceramics*, A.M. Alper (ed.), p. 127, Academic Press, San Diego, (1995).

[95Vil] P. Villars, A. Prince, H. Okamoto, "Handbook of Ternary Alloy Phase Diagrams," Vol. 3, ASM International, (1995).

[95Wen] R.M. Wentzcovitch, N.L. Ross, and G.D. Price, Phys. Earth Planet. Inter 90 (1995) 101.

[96Agr] J. Ågren, "Multicomponent Diffusion in Compound Steel," in: *The SGTE Casebook*, K. Hack (ed.), p. 209, The Institute of Materials, London, (1996).

[96Ann] S. Annaji, R.Y. Lin, and S.K. Wu, "Joining of Titanium Aluminides using Al-foil," in: Design Fundamentals of High Temperature Composites, Intermetallics and Metal-Ceramic Systems, R.Y. Lin, Y.A. Chang, R.G. Reddy, and C.T. Liu (eds.), p. 125, The Minerals, Metals & Materials Society, Warrendale, PA., (1996).

[96Bal] R.G.J. Ball, P.K. Mason, and M.A. Mignanelli, "Application of Phase Equilibrium Calculations to the Analysis of Severe Accidents in Nuclear Reactors," in: *The SGTE Casebook*, K. Hack (ed.), p. 135, The Institute of Materials, London, (1996).

[96Bar1] T.I. Barry and A.T.Dinsdale, "Hot Salt Corrosion of Superalloys," in: *The SGTE Casebook*, K. Hack (ed.), p. 56, The Institute of Materials, London, (1996).

[96Bar2] T.I. Barry, A.T. Dinsdale, S.M. Hodson, and J.R. Taylor, "Pyrometallurgy of Copper-Nickel-Iron Sulphide Ores: The Calculation of Distribution of Components between Matte, Slag, Alloy and Gas Phases," in: *The SGTE Casebook*, K. Hack (ed.), p. 151, The Institute of Materials, London, (1996).

[96Bel] A. B. Belonoshko and L. S. Dubrovinsky, Geochim. Cosmochim. Acta 60 (1996) 1645.

[96Bha] K. Bhanumurthy and R. Schmid-Fetzer, Mater. Sci. Eng. A A220 (1996) 35.

[96Cha] C.H. Chang, A. Davydov, B.J. Stanbery, and T.J. Anderson, "Thermodynamic Assessment of the Cu-In-Se System and Application to Thin Film Photovoltaics," in: *Proc. 25th PVSC*, p. 849, (1996).

[96Cra] M.B. Crawford, Comp. Geosci. 22 (1996) 109.

[96Eng] A. Engström, "Long range diffusion and microstructural evolution in multiphase alloys," Thesis, KTH, Sweden (1996).

[96Eri] G. Eriksson and K. Hack, "Production of Metallurgical Grade Silicon in an Electric Arc Furnace," in: *The SGTE Casebook*, K. Hack (ed.), p. 200, The Institute of Materials, London, (1996).

[96Fer] A. Fernández Guillermet, "Using Calculated Phase Diagrams in the Selection of the Composition of Cemented WC Tools with a Co-Fe-Ni Binder Phase," in: *The SGTE Casebook*, K. Hack (ed.), p. 77, The Institute of Materials, London, (1996).

[96Gus] P. Gustafson, "Computer Assisted Development of High Speed Steels," in: *The SGTE Casebook*, K. Hack (ed.), p. 70, The Institute of Materials, London, (1996).

[96Hac] K. Hack (ed.), "The SGTE Casebook," The Institute of Materials, London, (1996).

[96Hil1] M. Hillert and C. Qiu, "Prediction of Loss of Corrosion Resistence in Austenitic Stainless Steels," in: *The SGTE Casebook*, K. Hack (ed.), p. 85, The Institute of Materials, London, (1996).

[96Hil2] M. Hillert and S. Jonsson, "Prediction of a Quasitenary Section of a Quaternary Phase Diagram," *The SGTE Casebook*, K. Hack (ed.), p. 99, The Institute of Materials, London, (1996).

[96Hol] T. Holm and J. Ågren, "The Carbon Potential during Heat Treatment of Steel," in: *The SGTE Casebook*, K. Hack (ed.), p. 176, The Institute of Materials, London, (1996).

[96Kao] C.R. Kao, J. Woodford, and Y.A. Chang, "Reactive Diffusion between Silicon and Niobium Carbide, Application to the *in-situ* Synthesis of Silicon carbide / Niobium Disilicide Composite," in: *Design Fundamentals of High Temperature Composites, Intermetallics and Metal-Ceramic Systems*, R.Y. Lin, Y.A. Chang, R.G. Reddy, and C.T. Liu (eds.), p. 3, The Minerals, Metals & Materials Society, Warrendale, PA, (1996).

[96Kat] U.R. Kattner, W.J. Boettinger, and S.R. Coriell, Z. Metallkde. 87 (1996) 522.

[96Kor] J. Korb and K. Hack, "Calculation of the Concentration of Iron and Copper Ions in Aqueous Sulphuric Acid Solutions as a Function of the Electrode Potential," in: *The SGTE Casebook*, K. Hack (ed.), p. 118, The Institute of Materials, London, (1996).

[96Kou] A. Koukitu, N. Takahashi, T. Taki, and H. Seki, Jpn. J. Appl. Phys. 35 (1996) L673.

[96Miz] S. Mizoguchi, "A study on segregation and oxide inclusions for the control of steel properties," University of Tokyo, Tokyo, (1996).

[96Nic] K.G. Nickel, H.L. Lukas, and G. Petzow, "High Temperature Corrosion of SiC in Hydrogen-Oxygen Environments," in: *The SGTE Casebook*, K. Hack (ed.), p. 163, The Institute of Materials, London, (1996).

[96Pau] M. Paulasto, F.J.J. van Loo, and J.K. Kivilahti, "On the Metallurgy of Active Brazing of Silicon Nitride," in: *Design Fundamentals of High Temperature Composites, Intermetallics and Metal-Ceramic Systems*, R.Y. Lin, Y.A. Chang, R.G. Reddy, and C.T. Liu (eds.), p. 113, The Minerals, Metals & Materials Society, Warrendale, PA, (1996).

[96Ric] A. von Richthofen and R. Domnick, Thin Solid Films 283 (1996) 37.

[96Sax] S.K. Saxena, Geochim. Cosmochim. Acta 60 (1996) 2379.

[96Sch] R. Schmid-Fetzer, "Fundamentals of Bonding by Isothermal Solidification for High Temperature Semiconductor Applications," in: *Design Fundamentals of High Temperature Composites, Intermetallics and Metal-Ceramic Systems*, R.Y. Lin, Y.A. Chang, R.G. Reddy, and C.T. Liu (eds.), p. 75, The Minerals, Metals & Materials Society, Warrendale, PA, (1996).

[96Sei1] H.J. Seifert and F. Aldinger, Z. Metallkde. 87 (1996) 841.

[96Sei2] H.J. Seifert, H.L. Lukas, and G. Petzow, "Computational Thermodynamics in Materials Science," in: *Design Fundamentals of High Temperature Composites, Intermetallics and Metal-Ceramic Systems*, R.Y. Lin, Y.A. Chang, R.G. Reddy, and C.T. Liu (eds.), p. 297, The Minerals, Metals & Materials Society, Warrendale, PA, (1996).

[96Sui] H. Suito and R. Inoue, ISIJ International 36(5) (1996) 528.

[96Tur] E. Turkdogan, "Principles of Steelmaking," The Institute of Materials, London, (1996).

[96Vah] C. Vahlas, C. Bernard, and R. Madar, "The Thermodynamic Simulation in the Service of the CVD Process. Application to the Deposition of $WSi_2$ Thin Films," in: *The SGTE Casebook*, K. Hack (ed.), p. 108, The Institute of Materials, London, (1996).

[96Wei] F. Weitzer, P. Rogl, F.H. Hayes, J.A.G. Robinson, in: *Werkstoff Woche '96, Materialwissenschaftliche Grundlagen*, F. Aldinger and H. Mughabri (eds.), p. 185, Deutsche Gesellschaft für Materialkunde, (1997).

[97Ban] D.K. Banerjee, M.T. Samonds, U.R. Kattner, and W.J. Boettinger, "Coupling of Phase Diagram Calculations for Multicomponent Alloys with Solidification Micromodels in Casting Simulation Software," In: *SP97 Proc. 4th Intl. Conf. Solidification Processing*, J. Beech and H. Jones (eds), p. 354, University of Sheffield, UK, (1997).

[97Eri] G. Eriksson, P.J. Spencer, and D. Neuschütz, "Comparison of calculated and experimental dioxin levels in the off-gas of a sinter plant," in: *High Temperature Chemistry IX*, K.E. Spear (ed.), p. 278, The Elecrochemical Society, (1997).

[97Ghi] M.S. Ghiorso, Ann. Rev. Earth Planet. Sci. 25 (1997) 221.

[97Got] M. Gottschalk, Eur. J. Mineral. 9 (1997) 175.

[97Hil] M. Hillert, B. Burton, K. S. Saxena, S. Degterov, K.C. Hari Kumar, H. Ohtani, F. Aldinger, and A. Kussmaul, CALPHAD 21 (1997) 247.

[97Kra] T. Kraft and Y.A. Chang, JOM 49(12) (1997) 20.

[97Lee1] B.-J. Lee, N.M. Hwang, and H.M. Lee, Acta Mater. 45 (1997) 1867.

[97Lee2] B.-J. Lee, Acta Mater. 45 (1997) 3993.

[97Meu] B. Meurer, P. Spencer, and D. Neuschütz, J. Chim. Phys. 9 (1997) 889.

[97Oer] L.C. Oertel and A. Costa e Silva, "Applications of thermodynamic modeling in the prediction of slag-metal equilibrium in steelmaking" (in portuguese). XXVIII Seminário sobre Fusão, Refino e Solidificação dos Aços, Campinas, SP, Campinas, SP, ABM, São Paulo, SP, (1997).

[97Sch] M.C. Schneider, J.P. Gu, C. Beckermann, W.J. Boettinger, and U.R.Kattner, Metall. Mater. Trans. A 28A (1997) 1517.

[97Swa] V. Swamy and L. S. Dubrovinsky, Geochim. Cosmochim. Acta 61 (1997) 1181.

[97Tut] A.V. Tutbalin and D.V. Grichuk, Geochem. Intern. 35 (1997) 972.

[97Yoo] S.-W. Yoon, J.R. Soh, H.M. Lee, and B.-J. Lee, Acta Mater. 45 (1997) 951.

[98Ans] I. Ansara, A.T. Dinsdale, M.H. Rand, "COST 507: Definition of Thermochemical and Thermophysical Properties to Provide a Database for the Development of New Light Alloys," Vol. 2, European Commission, DG XII, Brussels, (1998).

[98Bra1] J. Brandt and L. Nilsson, MECH. COHES.-FRICT. MATER. 3(1998).

[98Bra2] J. Brandt, "On constitutive modelling of the compaction and sintering of cemented carbides," Thesis, Linköping University, Sweden (1998).

[98Buc] F.v. Buch, B.L. Mordike, A. Pisch, and R. Schmid-Fetzer, Mater. Sci. Eng. A (1998) accepted.

[98Cas] R. N. Castro and A. Costa e Silva, "Dynamic modeling of mixed blow converter (in portuguese)," to be published in XXIX Seminário sobre Fusão, Refino e Solidificação dos Aços, SP, Sao Paulo, Brasil, ABM, São Paulo, SP (1998).

[98Cha] T.G. Chart, "A Summary of the COST 507 Action and Examples of Practical Applications of the Database," in: *COST 507: Definition of Thermochemical and Thermophysical Properties to Provide a Database for the Development of New Light Alloys*, Vol. 1, p. 15, European Commission, DG XII, Brussels, (1998).

[98Che] Q. Chen, M. Hillert, B. Sundman, W.A. Oates, S.G. Fries, and R. Schmid-Fetzer, J. Electron. Mater. 27 (1998) 961.

[98Cre] R. Cremer, M. Witthaut, and D. Neuschütz, in: *Value Addition Metallurgy*, W.D. Cho, and H.Y. Sohn (eds.), p. 249, The Minerals, Metals & Materials Society, (1998).

[98Gra] U. Grafe, D. Ma, A. Engström,, and S.G. Fries, "Calculation of Microsegrgation for the Directionally Solidified SuperAlloy CMSX 4 using a Pseudo 2-Dimensional Model," in: *Modeling of Casting, Welding, and Advanced Solidification Processes VIII*, B.G. Thomas, and C. Beckermann (eds.), p. 227, The Mineral, Metals & Materials Society, (1998).

[98Dav] R. H. Davies, A. T. Dinsdale, J. A. Gisby, "MTDATA Handbook: Application Interface Programming Guide", CMMT, National PhysicalLaboratory, UK, (1998).

[98Jan] A. Jansson, T.G. Chart, "A Thermochemical Assessment of Data for the Al-rich Corner of the Al-Fe-Mn System, and a Revision of Data for the Al-Mn System," in: *COST 507: Definition of Thermochemical and Thermophysical Properties to Provide a Database for the Development of New Light Alloys*, Vol. 1, p. 257, European Commission, DG XII, Brussels, (1998).

[98McC] T.M. McCollom, and E.L. Shock, J. Geophys. Res. 103 (B1) (1998) 547.

[98Ran] M.H. Rand, P. Kolby, T.G. Chart, "A Thermochemical Assessment of Data for the Al-rich Corner of the Al-Mn-Si System," in: *COST 507: Definition of Thermochemical and Thermophysical Properties to Provide a Database for the Development of New Light Alloys*, Vol. 1, p. 246, European Commission, DG XII, Brussels, (1998).

[98Sch] R. Schmid-Fetzer and K. Zeng, Metall. Mater. Trans. A 28A (1997) 1949.

[98Sei] H.J. Seifert, H.L. Lukas, and F. Aldinger, Ber. Bunsenges. Phys. Chem. 102 (1998) 1309.

[98Spe] P.J. Spencer, G. Eriksson, and A.von Richthofen, in: *Proc. CODATA ' 94*, Chambéry, France, Sept. 1994, Springer, (1998).

[98Zen] K. Zeng, R. Schmid-Fetzer, and P. Rogl, J. Phase Equilibria 19 (1998) 124.